The Arizona Physiological Society

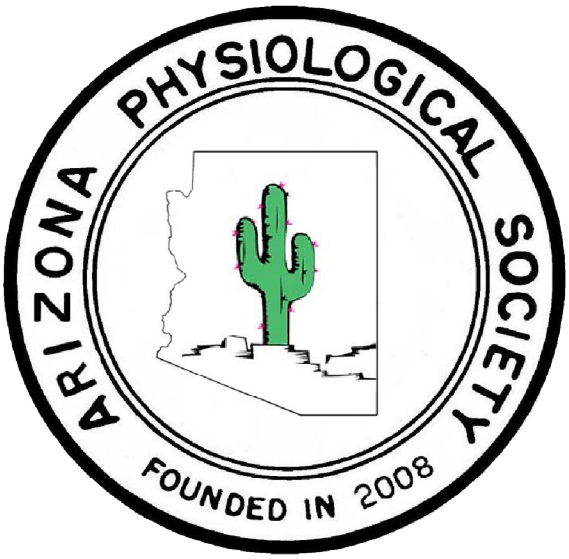

10th Annual Meeting
October 13-14, 2017

Northern Arizona University
(Flagstaff)
DuBois Ballroom

Sponsors and support

Pearson

VWR International LLC

American Physiological Society

ASU College of Health Solutions
ASU School of Life Sciences

University of Arizona

Midwestern University

Northern Arizona University Office of the Vice President for Research

Northern Arizona University Center for Bioengineering Innovation

PROGRAM
Arizona Physiological Society
10th Annual Meeting

All events will take place in the DuBois Ballroom, in building 64 on this map http://www2.nau.edu/nau-map/ , at 306 E Pine Knoll Dr. Please take the elevator or stairs to the second floor, where you will find the ballroom.

Friday, October 13, 2017

12:00 **Registration** opens

12:00 **Poster Set Up**

12:50 **Welcome to Meeting**
Kiisa Nishikawa, Northern Arizona University, President, AZPS

12:55 **Introduction of High School Teachers**
Tobias Riede, Midwestern University, Secretary/Treasurer, AZPS

1:00 – 1:45 Session I: Metabolic Physiology
Chair: TBD

1:00 – 1:15 **Michael Zawada**, Professor, A.T. Still University.
A Role for the Brain Renin-Angiotensin System (RAS) in Parkinson's, Alzheimer's, and Down Syndrome.

1:15 – 1:30 **Ryan Lord**, Medical student, Midwestern University.
Increased Serum GIP Levels Correlate to Improved Survival Rates in Female DF508-CF Mice Fed Dietary Genistein.

1:30 – 1:45 **Keane Urashima**, Graduate student, University of Arizona, Tucson.
Cytochrome C Oxidase is Differentially Methylated in Whole Blood from Participants with Metabolic Syndrome.

1:45 – 2:00 Break

2:00 – 2:45 Session II: Comparative Physiology
Chair: Karen Sweazea, President-elect, AZPS

2:00 – 2:15 **Jon Harrison**, Professor, Arizona State University.
Functional Hypoxia and HIF-Signaling Pre-Molting in *Drosophila.*

2:15 – 2:30 **Molly Shuman-Goodier**, Graduate student, Northern Arizona University.
Studying amphibian physiology to evaluate pesticide safety in rice fields.

2:30 – 2:45 **Victor Zhang**, Graduate student, Northern Arizona University.
Living on the Human-Wildlife Boundary: Determinants of Activity in Suburban Striped Skunks (*Mephitis mephitis*).

2:45 – 3:00 Break

3:00 – 3:45 **Session III: Musculoskeletal Physiology**
Chair: Uzma Tahir, Northern Arizona University

3:00 – 3:15 **Kathy Kuang**, Undergraduate student, University of Arizona, Tucson.
Obese versus Non-Obese Patients with Severe Low Back Pain during Gait.

3:15 – 3:30 **Anthony Hessel**, Graduate student, Northern Arizona University.
Twitch Contractions Are Impaired in Skeletal Muscles with a Titin Mutation.

3:30 – 3:45 **Alexander Pendleton**, Graduate student, University of Arizona, Tucson.
Impaired Satellite Cell Differentiation and Regulation in Lambs with Intrauterine Growth Restriction.

3:45 – 5:00 **Session IV: Cardiovascular Physiology**
Chair: Anthony Hessel, Northern Arizona University

3:45 – 4:00 **Alexandra Garvin**, Post-doctoral scholar, University of Arizona, Tucson.
Influence of Age and Ischemia on cardiac subsarcolemmal and interfibrillar mitochondrial function sensitizes the aged female rat heart to programmed necrosis.

4:00 – 4:15 **Brittney McCormick**, Graduate student, University of Arizona, Phoenix.
Impact of Bradykinin B1 Receptor Blockade on Angiotensin II-Induced Cardiac and Aortic Remodeling.

4:15 – 4:30 **Lakshmi Madhavpeddi**, Graduate student, University of Arizona.
Role of Angiotensin II in Cardiovascular Stress Responses in Rats Exposed to Glucocorticoids *in Utero*.

4:30 – 4:45 **Andrew Antolic**, Post-doctoral scholar, University of Arizona, Tucson.
Gene Expression in the Newborn Heart is Altered by Chronic Maternal Stress.

4:45 – 5:00 **Sanna Rahman**, Undergraduate student, University of Arizona, Phoenix.
Lenalidomide Attenuates High Fat Diet Induced Cyclooxygenase-2 Levels in Primary Human Vascular Smooth Muscle Cells.

5:00 – 5:15 Break

5:15 – 6:15 **Keynote speaker**
Dr. George Somero, David and Lucile Packard Professor in Marine Science, Emeritus, Stanford University.
"Molecular Adaptation to Environmental Stress: Intrinsic versus Extrinsic Solutions"
Introduced by **Kiisa Nishikawa** (Northern Arizona University)

6:30 – 7:30 **Dinner and Social**

7:30 – 8:00 **Informal Discussion** with Guest Teachers on Teaching of Physiology in Arizona High Schools

8:00 – 8:30 **Minute posters** (25 posters)
Introduced by **Anthony Hessel**, Graduate student, NAU

8:30 – 9:30 **Poster session I** (25 posters)

Saturday, October 14, 2017

7:30 – 8:30 **Continental breakfast**

8:30 – 9:15 Session V: Cutting-Edge Methods in Physiology
Chair: **Ann Revill,** Assistant Professor, Midwestern University

8:30 – 8:45 **Kevin Hoskins**, Undergraduate, Grand Canyon University and Isac Artzi, Associate Professor, Grand Canyon University.
3D Scanning of a Human Body for Dimensional Measurements and Detections of Changes.

8:45 – 9:00 **José Rosado-Toro**, Postdoctoral scholar, University of Arizona, Tucson.
Feasibility of MRI-RHC Based Pressure Volume Loops in Control and PAH Patients.

9:00 – 9:15 **Jacob Campbell**, Graduate student, Arizona State University.
Non-conventional Anoxia Tolerance: Adult *Drosophila* Outlive Larvae despite Inferior ATP and Hemolymph K+ Maintenance.

9:15 – 9:30 **Session VI: History of Physiology**
Chair: Stan Lindstedt, Professor Emeritus, NAU

9:15 – 9:30 **Charles Tipton**, Professor Emeritus, University of Arizona.
What I Failed to Learn in Kindergarten or Graduate School Concerning the History of Physiology.

9:30 – 9:45 Break

9:45 – 10:45 **Arizona Distinguished Lecture**
Dr. Janis Burt, Professor, Department of Physiology, University of Arizona.
"An Integrative Approach to Defining the Role of Connexins in Vascular Development and Remodeling".
Introduced by **John Kanady**, Councillor, AZPS, University of Arizona, Tucson.

10:45 – 11:15 **Minute posters** (24 posters)
Introduced by **Anthony Hessel**, Graduate student, NAU

11:15 – 12:15 **Poster session II** (24 posters)

12:15 – 1:00 **Lunch**

1:00 – 1:45 **Business Meeting**

1:45 Adjourn

Posters: alphabetical by lead author—Friday posters

Number	Last name	First name	Title	Keywords
F1	Alexander	Tia	Combination of mild aerobic exercise and angiotensin-II type-I receptor blocker treatment on cardiac and aortic function in a mouse model of Marfan Syndrome.	Marfan's Syndrome, Aortic Aneurysm, Exercise
F2	Antolic	Andrew	Gene expression in the newborn heart is altered by chronic maternal stress	Fetus Pregnancy Stress Microarray
F3	Broderick	Tom L.	Characterization of cardiac and aortic function and structure by high resolution ultrasound imaging in the 3xTg mouse model of Alzheimer's Disease.	Alzhiemer's, cardiac, aorta, 3xTg
F4	Clark	William	Consumption of a Refined Carbohydrate Diet Does Not Impair Vasodilation of Cranial Tibial Arteries from Mourning Doves (Zenaida macroura)	Glucose Regulation, Mourning Doves, Carbohydrate, Cranial Tibial, Vasodilation
F5	Cogley	Theodore	Oxygen-limitation in developing tobacco hornworm caterpillars, Manduca sexta	Hypoxia, Development, Oxygen
F6	Dutta	Samrat	Calcium dependent interaction between N2A-Halo and F-actin: a single molecule study	Titin, Actin, Biophysics
F7	Garvin	Alexandra	Influence of age and ischemia on cardiac subsarcolemmal and interfibrillar mitochondria function and morphology in a novel model of estrogen deficiency	heart, ischemic injury, mitochondria, programmed necrosis
F8	Hessel	Anthony	Twitch contractions are impaired in skeletal muscles with a titin mutation.	titin, isometric force production, force transmission
F9	Hoskins	Kevin	3D scanning of a human body for dimensional measurements and detection of changes	3-D Scan, Body Segments, Bodily Abnormailities, Image Processing
F10	Hoxha	Brikena	Evaluation of the effects of methyl-β-cyclodextrin on aortic function & structure in a mouse model of Marfan syndrome using high frequency ultrasound imaging.	Marfan Syndrome, heart, aorta, methyl-β-cyclodextrin
F11	Huck	Thomas	Quantifying the Balance and Stability of a Powered Ankle-Foot Prosthesis using a Bio-Inspired Controller	Titin, Winding Filament Hypothesis, Lower limb prosthesis, gait analysis, whole-body angular momentum
F12	Kuang	Kathy	OBESE VERSUS NON OBESE PATIENTS WITH SEVERE LOW BACK PAIN DURING GAIT	Gait ,Obesity, Low back pain
F13	Madhavpeddi	Lakshmi	Role of Angiotensin II in Cardiovascular Stress Responses in Rats Exposed to Glucocorticoids In Utero	Dexamethasone, Fetal Programming, Cardiovascular Disease, Angiotensin II
F14	Mayra	Selicia	Comparison of High-Nitrate versus Low-Nitrate Diets on Cardiovascular Health in Post-Menopausal Women	High nitrate, Cardiovascular health, Post-menopausal women, endothelial function, blood pressure
F15	McCormick	Brittney	Impact of Bradykinin B1 Receptor Blockade on Angiotensin II-Induced Cardiac and Aortic Remodeling	Hypertension, Angiotensin II, Bradykinin, Cardiovascular Remodeling, Inflammation
F16	Pendleton	Alexander	IMPAIRED SATELLITE CELL DIFFERENTIATION AND REGULATION IN LAMBS WITH INTRAUTERINE GROWTH RESTRICTION	SMAD4, TGFB, satellite cell, muscle
F17	Perez	Octavio	Impact of Prior ACE Inhibition on Cardiac Fibroblast Physiology	cardiac, fibroblasts, ACE inhibitor, proliferation
F18	Revill	Ann	Noradrenergic and cholinergic modulation of Dbx1 XII inspiratory premotoneurons	Hypoglossal premotoneuron, Dbx1, airway control, acetylcholine, noradrenaline
F19	Riede	Tobias	Ultrasonic vocalization and physiological responses in rats	vocal behavior, respiration, autonomic nervous system
F20	Rosado-Toro	Jose	Feasibility of MRI-RHC based pressure volume loops in control and PAH patients	Ventricular Functional Analysis, Right Ventricle, MRI
F21	Sargent	James	Accumulation of Gut Bacteria May Cause the Age-Related Decline of Anoxia Tolerance in Adult Drosophila melanogaster	Anoxia, hypoxia, aging, mirobiome, bacteria
F22	Shi	Sam	Differential sphingosine-1-phosphate receptor 1 expression following middle cerebral artery occlusion in murine heart and brain	sphingosine-1-phosphate receptor 1, ischemic brain injury, stroke
F23	Talley	Nicholas	Role of Inducible Nitric Oxide Synthase (iNOS) in Marfan Syndrome Associated Aortic Aneurysm	Marfan Syndrome, iNOS, Thoracic Aorta
F24	Weimer	Erik	3D scanning of a human body for dimensional measurements and detection of changes	3D Scan, Body Segments, Bodily Abnormalities, Image Processing
F25	Zapata Bustos	Rocio	Reduced skeletal muscle transcription factor expression response to exercise in insulin resistance	transcription factors, insulin resistance, exercise

Posters: alphabetical by lead author—Saturday posters

Number	Last name	First name	Title	Keywords
S1	Artzi	Isac	3D scanning of a human body for dimensional measure*Erikments and detections of changes	3D scan, body segments, bodily abnormalities, image processing
S2	Basile	Anthony	Relationship between animal class and dietary profile on blood glucose concentrations	Blood Glucose, Evolution, Taxonomy
S3	Chandrashekar	Archana	Genistein-induced weight loss in ob/ob diabetic mice is associated with reductions in serum metabolic and cytokine markers	diabetes, mouse, ob/ob
S4	Chung	Su	The function of the CD47 and NO/cGMP signaling in tumor progression	cancer, immune surveillance, signaling pathways
S5	Cotter	Maura	The lipidated connexin mimetic peptide, SRPTEKT-Hdc, is a potent inhibitor of Cx43-mediated intercellular communication with specificity for the pS368 phospho-form	Gap junction channel inhibitor, Lipidated connexin mimetic peptide, SRPTEKT-Hdc, Connexin 43, S368 phospho-form
S6	Crawford	Melisa	NOVEL ORGANOMETALLIC COMPLEX LOWERS NON-HDLc IN MALE ADOLESCENT RATS FOLLOWING 10-WEEK HIGH FAT DIET	high fat diet, adolescents, metabolic disorders
S7	DeLucia	Claire	Respiratory muscle training impacts daytime and overnight blood pressure in adults with obstructive sleep apnea	Respiratory muscle training, blood pressure, sympathetic nerve activity, obstructive sleep apnea, baroreflex sensitivity
S8	Ek-Vitorin	Jose	Comparison of two phospho-mimic mutations of Cx43 with opposite arrhythmogenic potential	Gap junction, Connexin, arrhythmia, channels
S9	Fox	Trevor	Respiration is a one way street: Abdominal pumping induces unidirectional flow in beetles	Respiration Insects air flow respirometry
S10	Gonzales	Rayna	Doxorubicin temporally modules cyclooxygenase-2 levels in human vascular smooth muscle cells	doxorubicin, vascular smooth muscle, inflammation, cyclooxygenase-2
S11	Gu	Haiwei	Targeted Metabolic Profiling of Bile Acids in Breast Cancer Patients	bile acids, breast cancer, LC–MS/MS, targeted metabolic profiling, metabolomics
S12	Kellermayer	Dalma	Function of novex-3, the tiny titin in cardiac and skeletal muscle	titin, TTN gene, novex-3, obscurin
S13	Kras	Katon	Proteome differences of subsarcolemmal and intermyofibrillar mitochondria reveal energy metabolism redistribution in skeletal muscle of obese subjects	Obesity, skeletal muscle, mitochondria, proteomics
S14	Lord	Ryan	INCREASED SERUM GIP LEVELS CORRELATE TO IMPROVED SURVIVAL RATES IN FEMALE DF508-CF MICE FED DIETARY GENISTEIN	genistein, CF, mouse, intestine
S15	Miyano	Carissa	Heat production deficiencies in the muscular dystrophy with myositis (mdm) mouse	thermoregulation, metabolic rate, nonshivering thermogenesis
S16	Ojameruaye	Ochuko	Effects of Detraining and Retraining in a Follow-Up Cohort With Type 2 Diabetes	aerobic capacity, deconditioning, high intensity interval training, type 2 diabetes
S17	Olson	Christopher	GABAergic neurons in vocal- and non-vocal learning hummingbirds	hummingbird, songbird, GABA, vocal learning
S18	Pasch	Bret	An extended matched filter between call frequency and auditory sensitivity in northern grasshopper mice	acoustics, behavior, communication, sensory systems
S19	Rahman	Sanna	Lenalidomide attenuates high fat diet induced cyclooxygenase-2 levels in primary human vascular smooth muscle cells	lenalidomide, cyclooxygenase-2, vascular smooth muscle, high fat diet
S20	Shuman-Goodier	Molly	Studying amphibian physiology to evaluate pesticide safety in rice fields.	amphibian, pesticide, thyroid
S21	Urashima	Keane	Cytochrome C Oxidase is Differentially Methylated in Whole Blood from Participants with Metabolic Syndrome	Methylation, Blood, Metabolic SYndrome, AIR Registry
S22	Whitney	Christopher	Predicting in vivo muscle force in running guinea fowl using a muscle model based on the winding filament hypothesis.	Muscle modeling, simulation, high performance computing
S23	Wilson	Tomoko	Troponin I phosphorylation in diabetic and non-diabetic hearts	Troponin I, diabetes, phosphorylation
S24	Zawada	Michael	A Role for the Brain Renin-Angiotensin System (RAS) in Parkinson's, Alzheimer's, and Down syndrome	angiotensin, interleukin, neuroinflammation, oxidative stress, Parkinson's

FRIDAY PRESENTATIONS

F1. Combination of mild aerobic exercise and angiotensin-II type-I receptor blocker treatment on cardiac and aortic function in a mouse model of Marfan Syndrome.

***Alexander T, College of Health Sciences, Midwestern University, Glendale, AZ** , Hoxha B, College of Health Sciences, Midwestern University, Glendale, AZ , Talley NA, College of Health Sciences, Midwestern University, Glendale, AZ , Cameron E, College of Medicine, Midwestern University, Glendale, AZ , Cooper K, College of Health Sciences, Midwestern University, Glendale, AZ , Broderick TL, College of Medicine, Midwestern University, Glendale, AZ , Vallejo-Elias J, College of Medicine, Midwestern University, Glendale, AZ , Esfandiarei M, College of Health Sciences, Midwestern University, Glendale, AZ

Marfan syndrome (MFS) is a connective tissue disorder that causes complications throughout the body. However, the cardiovascular effects of MFS, specifically aortic aneurysms, are the leading cause of morbidity and mortality in patients. Both the transforming growth factor beta (TGF-β) and angiotensin II type I receptor (AT1R) signaling pathways are known to contribute to the progression of MFS aneurysms. Recently, our laboratory reported that low-intensity mild exercise can improve aortic function and structure in the mouse model of MFS. Losartan, an AT1R blocker, has been shown to slow down the progression of MFS aneurysms in both the mouse model and human patients. Hence, it is a preferred drug therapy used to in MFS patients. In this study, we have explored the potential of a combinational therapy of exercise and losartan in a well-established mouse model of MFS associated aortic aneurysm in order to determine if there are additive protective and delaying effects on the progression of aortic aneurysm in the mouse. Treatment consisted of 0.6g/L (full dose) or 0.3g/L (half dose) of losartan in drinking water combined with a 55% VO2 max exercise regimen (30min/day, 5days/week). Mice were divided in experimental groups: control, MFS, MFS + Exercise, MFS + 0.6g/L losartan, MFS + 0.3g/L losartan, MFS + Exercise + 0.6g/L losartan, and MFS + Exercise + 0.3g/L losartan. The biophysical properties of the aorta, such as the aortic diameter and pulse wave velocity (PWV), were determined by Vevo 2100 high resolution ultrasound imaging system (FUJIFILM VisualSonics) in 3-month-old MFS mice. Aortic diameter, expressed as aortic annulus, sinotubular junction, and sinus of Valsalva, were not significantly different among experimental groups. However, MFS mice exhibited higher PWV as compared to control mice, indicating increased stiffness of aortic wall in these mice. For cardiac function and structure, echocardiographic measurements of left ventricular dimension, interventricular septum in systole and diastole, cardiac output, stroke volume, ejection fraction, early (E), and atrial (A) ventricular filling velocities, and E/A ratio, demonstrated no significant differences between the groups. , The continuation of the longitudinal study at 6 and 9 months of age and as the aneurysm progresses, we will be able to continue our evaluation of aortic and cardiac function and structure in MFS mice subjected to exercise only, losartan only, or the combinational therapy.

Funding: Midwestern University Biomedical Sciences Program

F2. Gene expression in the newborn heart is altered by chronic maternal stress

Antolic A, University of Florida, Gainesville, FL , Curtis C, University of Florida, Gainesville, FL , Keller-Wood M, University of Florida, Gainesville, FL

Previous studies from our lab that focused on effects of maternal stress in late gestation found increases in fetal heart thickness, heart weight, and apoptosis in Purkinje fibers after an infusion of cortisol (1 mg/kg/day) for 15 days into pregnant ewes starting at 115 days of gestation (CORT). When CORT exposure continued until term (~145 days of gestation) in this model, there was a profound increase in perinatal stillbirth, suggesting that prior changes in the fetal heart and conduction system could contribute to the stillbirth. Transcriptomic analysis of term fetal hearts indicated cardiac metabolic pathways and mitochondria were affected by CORT. Recently, we have demonstrated that chronic CORT significantly reduces fetal heart rate and mean aortic pressure and increases the

duration of the P wave and PR interval of the fetal ECG on the day of birth. , Left ventricle (LV) samples were collected at necropsy from control (n=5) and CORT (n=5) newborn lambs. RNA was extracted, labeled, and hybridized to an Agilent ovine microarray. Differentially regulated genes (DEG) were identified using empirical a Bayes moderated t-test in R software. Global and detailed gene ontology and KEGG pathways were revealed using ClueGO in Cytoscape software. Western blot and histological (PicroSirius Red staining) techniques were used to validate results from the microarray. , 386 genes were significantly DEG by CORT in the LV, 166 genes were upregulated, and 220 genes were downregulated. ClueGO identified pathways and terms associated with genes relating to cardiac myofibril assembly and development (SMAD2, SMAD4, BMP4, MYOD1), calcium ion homeostasis (ATP2A2), mitochondrial function (PNPT), and malate metabolism (SLC25A10, SLC25A11). Based on these findings we performed western blot to quantitate mitochondrial electron transport chain proteins and histology for collagen deposition. Cytochrome c oxidase subunit 4 was significantly downregulated by CORT (2249.8□584.9 vs 1007.5□285.8 AFU). CORT also significantly increased collagen deposition in the LV (1.6%□0.3% vs 3.5%□0.9%). , The results from this study indicate that at birth, genes involved in cardiac ion homeostasis, metabolism, and structure are affected by CORT. Early and increased fetal exposure to cortisol causes cardiac mitochondrial dysfunction and collagen deposition, endangering the fetus' ability to survive the perinatal period, consistent with the ECG results observed at birth.

Funding: National Institutes of Health, HD057871, American Heart Association, 14GRNT20420048

F3. Characterization of cardiac and aortic function and structure by high resolution ultrasound imaging in the 3xTg mouse model of Alzheimer's Disease.

***Hoxha B, College of Health Sciences, Midwestern University, Glendale, AZ ,** Anderson MR, College of Medicine, Midwestern University, Glendale, AZ , Talley NA, College of Health Sciences, Midwestern University, Glendale, AZ , Alkhouli MF, College of Medicine, Midwestern University, Glendale, AZ , Squire MA, College of Medicine, Midwestern University, Glendale, AZ , Lopaschuk GD, University of Alberta, Edmonton, AB , Esfandiarei M, College of Health Sciences, Midwestern University, Glendale, AZ , Broderick TL, College of Medicine, Midwestern University, Glendale, AZ

Alzheimer's disease (AD) is a devastating neurodegenerative disease and recent clinical studies have demonstrated that patients with AD exhibit compromised cardiac function. In this study, we investigated whether the widely-used 3x-Tg mouse model of AD also presents with cardiovascular dysfunction. This model develops age-related neuropathology including plaques and tangles associated with synaptic dysfunction, and amyloid-beta deposits in the frontal cortex by six months. In vivo cardiovascular function, determined by echocardiography, was performed in seven-month-old male 3xTg mice (n=7) and age-matched controls (n=8) under isoflurane-induced anesthesia. While body weight was significantly lower in AD mice compared to control mice, no differences in heart weight were observed between groups. Measurement of aortic structure by echocardiography, expressed as aortic annulus, sinus of Valsalva, and sinotubular junction indicated no differences between groups. Ventricular dimensions, measured as interventricular septal end diastole and end systole, were also similar in AD and control mice. However, in terms of indices of function, ejection fraction was lower in AD mice, whereas early (A) and late (E) atrial ventricular filling velocities, the E/A ratio, and mitral valve deceleration time were increased in AD mice compared to control mice. Pulse wave velocity in AD mice was increased, which is an indication of increased stiffness and reduced elasticity of the aortic wall. We also observed a significant increase in elastic fiber fragmentation within the media of the aortic wall, which was associated with overall decreased elastin content and fiber length. Aorta from AD mice also exhibited pronounced medial and adventitial wall thicknesses compared to control mice. Collectively, our results provide novel information on structural and functional properties of the heart and aorta in the 3x-Tg mouse model of AD.

Funding: Midwestern University Office of Research and Sponsored Programs, Diabetes Action Research and Education Foundation

F4. Consumption of a Refined Carbohydrate Diet Does Not Impair Vasodilation of Cranial Tibial Arteries from Mourning Doves (Zenaida macroura)

Clark WF, Arizona State University, Tempe, AZ, Sweazea KL, Arizona State University, Tempe, AZ

Plasma glucose concentrations in mourning doves are three times higher than healthy humans. Chronic hyperglycemia in mammals is positively correlated with increases in the production of reactive oxygen species (ROS), whereas vascular ROS in mourning doves are similar to levels measured in healthy rodents. This lack of augmented ROS production in the presence of such high plasma glucose may be due to abundant endogenous antioxidants in doves, such as uric acid and vitamin C. Therefore, we hypothesized that feeding doves a refined carbohydrate diet would not impair vasodilation. To examine this hypothesis, we captured 11 wild mourning doves on the Arizona State University Tempe campus using walk-in style funnel traps, and housed them for 5 weeks. Birds were acclimated for 1 week during which time they transitioned to either a nutritionally-balanced dove seed diet (SD) or a refined carbohydrate (WB; white sandwich bread) diet. Blood samples were collected from the brachial vein of birds upon arrival and at the end of the 4-week intervention for the measurement of plasma metabolites. At the end of the 4-week diet, birds were euthanized with an overdose of sodium pentobarbital (200 mg/kg) and cranial tibial arteries were isolated, cannulated with glass pipettes and pressurized in a vessel chamber. Isolated arteries were pre-constricted to 50% of the initial diameter by adding increasing doses of phenylephrine (PE) to the superfusate. Endothelium-mediated vasodilation was measured by adding acetylcholine (ACh) in a half log incremental concentrations (10-9 M to 10-5 M). There were no significant differences in vasodilation between SD and WB ($p > 0.05$). To examine the effects of captivity, the data was compared to prior studies of isolated arteries from wild mourning doves (WMD). Endothelium-dependent vasodilation of both groups of captive birds were significantly greater than WMD (SD vs. WMD, $p=0.009$; WB vs. WMD, $p <0.05$). Consistent with our hypothesis, refined carbohydrate consumption did not impair vasodilation. Moreover, captivity improved vasodilation when compared to wild doves regardless of diet type.

Funding: American Physiology Society

F5. Oxygen-limitation in developing tobacco hornworm caterpillars, Manduca sexta

***Cogley TR, Arizona State University, Tempe, AZ ,** Greenlee KJ, North Dakota State University, Fargo, ND , Lundquist TA, North Dakota State University, Fargo, ND , Harrison, JF, Arizona State University, Tempe, AZ

Arthropods such as insects must periodically shed their exoskeleton in order to grow, but we do not yet know the specific parameters that are sensed and cause molting. As the organisms form more tissue that require more oxygen, they may not adequately increase the size of their tracheal system, potentially leading to oxygen limitation which may play a role in triggering molting. To partially test this idea, we quantified gene expression of Hypoxia-Inducible Factor (HIF) alpha and beta, and concentrations of the anaerobic metabolite lactate in tobacco hornworm caterpillars, Manduca sexta, both early and late within those developmental stages. We predicted that if oxygen-limitation occurs late in the instar that we would find an increase in HIF gene expression and lactate concentrations at that time. For the fifth instar, where the most growth and development occurs, we also quantified lactate concentrations during the wandering phase, where the fifth instar larva stops eating and tries to burrow in preparation for pupation. For gene expression quantification, RNA was isolated and relative gene expression quantified with qPRC. For lactate assays, animals were homogenized in perchloric acid and lactate concentrations measured with a spectroscopic assay. Expression of both HIFalpha and beta was higher at the end relative to the beginning of the 2, 3rd and 4th instar, but not for the 5th instar. Lactate concentrations were higher in the wandering phase of the fifth instar than in the earlier phases of the fifth instar, but did not differ

between early and late 4th instar animals. The increase in HIF gene expression and lactate concentrations later in some instars was consistent with the hypothesis of oxygen-limitation developing late in the instar; however, the inconsistency of the HIF and lactate results in different instars suggests instar-specific responses. Supported by NSF IOS 1256745.

Funding: NSF IOS 1256745

F6. Calcium dependent interaction between N2A-Halo and F-actin: a single molecule study

***Dutta Samrat, Northern Arizona University, Flagstaff, AZ ,** Nelson Brent, Northern Arizona University, Flagstaff, AZ , Gage Matthew, University of Massachusetts, Lowell, MA , Nishikawa Kiisa, Northern Arizona University, Flagstaff, AZ

In the last two decades, the role of titin's I-band region in muscle contraction has become clearer. It was shown that a mouse mutation with a deletion of the N2A domain from titin's I-band region reduces active stiffness and force production in whole skeletal muscles and myofibrils. Previous studies from our own and other laboratories also suggested an interaction between titin and actin. However, these studies did not report the forces associated with single titin-actin interactions in the presence of mechanical force and calcium. Here, we used AFM force spectroscopy to probe the interaction strength between a recombinant N2A-HALO construct and actin filament (F-actin). We performed AFM single molecule dynamic force spectroscopy (DFS) to measure the mechanical interaction strength of single N2A-HALO molecules with F-actin, in the presence and absence of calcium (pCa = 4.0). An N2A-Halo construct was expressed, consisting of the N2A region of titin (Ig80-IS-Ig81-Ig82-Ig83, where IS is the 117 amino acid insertion sequence) with a C-terminal Halo-tag sequence and N-terminal cysteines. The construct was immobilized on an amino-functionalized AFM cantilever tip. The interaction strength between this construct and actin filament was determined by probing the molecule during multiple approach-retraction cycles over various locations on a lipid-bilayer substrate functionalized with actin filaments. DFS was performed at physiological pulling rates (300-1000 nm/sec). Our preliminary data show that both the yield and strength of N2A-Halo interactions with F-actin nearly doubled in the presence of Ca2+, with multiple peaks at 50 ± 25 pN, 75 ± 10 pN, and 100 ± 25 pN in the rupture force distribution. Also, the force extension curves showed different rupture lengths. These results indicate multiple actin binding sites on the N2A-HALO construct. No significant interactions occurred between N2A constructs and the charged lipid bi-layer surface in the absence of F-actin. DFS experiments show that calcium increases the interaction probability and binding strength between N2A-Halo and F-actin under mechanical force. The measured N2A-Halo:actin interaction forces in the presence of calcium support a physiological role for titin in active muscle contraction and force enhancement, which confirms the usefulness of AFM in measuring single titin:actin interactions.

Funding: W. M. Keck Foundation and the Technology Research Initiative Fund of Northern Arizona University

F7. Influence of age and ischemia on cardiac subsarcolemmal and interfibrillar mitochondrial function sensitizes the aged female rat heart to programmed necrosis

***Garvin AM, The Pennsylvania State University, University Park, PA ,** Aurigemma NC, The Pennsylvania State University, University Park, PA , Korzick DH, The Pennsylvania State University, University Park, PA

Altered mitochondrial respiration (MR), calcium retention capacity (CRC), and morphology contribute to cardiac cell death mechanisms exacerbated by aging in males. The present study aimed to determine changes in mitochondrial morphology and subpopulation function with age and ischemia/reperfusion (I/R) injury in the female heart with specific attention to the contribution of programmed necrosis (PN) to cell death. A novel model

to recapitulate human menopause/age interactions was used in F344 female rats ovariectomized (OVX) at 15mo and studied at 24mo (MO OVX; n=32), vs adult (6mo; n=36). Rats were subjected to in vivo coronary artery ligation (CAL) and studies were performed at varying reperfusion times. MR and CRC were assessed in isolated subsarcolemmal (SSM) and interfibrillar (IFM) mitochondria following CAL (31 min I and 10 min R) or sham. Left ventricular tissue was imaged by transmission electron microscopy to evaluate mitochondrial area following CAL (31 min I and 10 min, 6 hr, or 24 hr R) or sham. Infarct size was determined by TTC staining with and without inhibition of PN using Nec-1 (CAL; 55 min I and 2 hr R). State 3 MR energized by either complex I (CI) or complex II (CII) substrates was selectively reduced by age in SSM ($p<0.02$), and by I/R in IFM ($p<0.05$). Although both adult and MO OVX mitochondria exhibit increased size during ischemia, presumably due to swelling, CRC was less in MO OVX vs. adult IFM with I/R (64%), suggesting earlier mitochondrial permeability transition pore (MPTP) opening in the aged. At CI, cyclosporine A (CsA) enhanced CRC 20% more in SSM and 74% more in IFM from adult compared to MO OVX suggesting reduced protective efficacy with age and MPTP involvement. Age induced a decrease in mitochondrial area and increases in cytosolic RIP1 and mitochondrial cyclophilin D suggesting age-associated alterations in mitochondrial dynamics and involvement of PN. As such, Nec-1 reduced infarct size, but a larger dose was necessary to achieve cardioprotection in the MO OVX suggesting an elevated contribution of PN to cardiac cell death with age. Following ischemia, adult mitochondria increase in size at 10 min and 6 hr R compared to sham, then return to baseline at 24 hr. Interestingly, MO OVX mitochondria do not increase in size until 6 hr of R persisting through 24 hr suggesting a shift in the time course of mitochondrial dynamics that may affect recovery. Our data suggest a sex-specific phenotype whereby reductions in both SSM and IFM function may play an additive role in the enhanced susceptibility to I/R injury and myocardial infarction in the aged female heart, which may predominantly occur by PN.

Funding: NHLBI, HL091097 , NIA, AG044132.

F8. Twitch contractions are impaired in skeletal muscles with a titin mutation.

***Hessel AL, Northern Arizona University, Flagstaff, AZ ,** Nishikawa KC, Northern Arizona University, Flagstaff, AZ

Twitch contractions, a muscle's response to a single electrical stimulus, are used to assess force production and transmission in skeletal muscle. Calcium release, cross bridge cycling and force transmission systems affect twitch properties in a quantifiable manner. Muscular dystrophy with myositis (mdm) is a mutation in mice that results in a small deletion in the N2A regions of titin in skeletal muscle, which decreases titin stiffness in active muscle. Although the mdm mutation has been shown to reduce force enhancement after stretch and isometric stress, few previous studies have assessed isometric contractile properties in more detail. We compared several twitch properties between extensor digitorum longus and soleus muscles from mdm and wild type mice, including electromechanical delay, rate of force development, time to peak force, maximum stress, half-relaxation time and total twitch time. The data were analyzed using two-way ANOVA with fixed effects of genotype, muscle and their interaction. The results indicated a significant genotype effect for all variables, with mdm muscles producing increased electromechanically delay, time to peak force, half-relaxation time and total twitch time, and decreases in maximum stress and rate of force development. These results suggest that the mdm mutation leads to a systemic impairment of isometric contractile function. For electromechanical delay, rate of force development, time to peak stress, and half-relaxation time, the differences between genotypes were consistently larger for the soleus than for the EDL, suggesting that EDL muscles may compensate for the mdm mutation better than soleus muscles. The increase in time to peak stress and half relaxation time strongly suggest that force transmission is impaired in muscles from mdm mice. It is also possible that force production may be impaired as well. Future work will assess cross bridge function directly by measuring ATP consumption in single fiber preparations.

Funding: This work was supported by the National Science Foundation [IOS-0732949, IOS-1025806, and IOS-1456868 to KCN], the W.M. Keck Foundation [KCN], and the ARCS Foundation [ALH].

F9. 3D scanning of a human body for dimensional measurements and detection of changes

***Weimer E, Grand Canyon University, Pheonix, AZ , *Hoskins K, Grand Canyon University, Pheonix, AZ,** Artzi I, Grand Canyon University, Pheonix, AZ

Purpose Statement: The feasibility of using an inexpensive 3D scanning system on a human body for dimensional measurements and subsequent detection of changes. , Materials/Methods: The materials used included a 3D StructureSensor, an iPad, laptop, Skanect software, and a mannequin. Our method makes an innovative use of 3D scanning and subsequent processing of captured data. First, we created 3D geometrical representations of body segments. Then we developed a mathematical model for representing the body segments. We also developed an algorithm which searches for those patterns within the dataset of body segments generated by the full body scan. When a match is found in the dataset, it means that a body segment has been identified. , Summary of Results: , We found an effective way of determining specific dimensions of a subject that was scanned. We developed a machine-learning based classifier software tool that categorizes human body segments after being presented with a large and diverse set of human bodies. The classifier implemented an adaptation of the k-means algorithm to automatically identify generic groups of subjects (body types). The resulting classification offered a reference framework for comparison with new scanned bodies. The high-resolution body scan enabled us to detect small differences between a scanned subject and the reference body segment. These differences can then be mapped onto known symptoms of various health problems, typically manifested as slight deformations of various body segments. , Conclusion: , Our approach shows promise in the identification of changes for multiple locations on the human body simply by performing a 3D scan of the subject, with a consistent and quantifiable degree of accuracy.

Funding: Grand Canyon University, Self-funded

F10. Evaluation of the effects of methyl-β-cyclodextrin on aortic function & structure in a mouse model of Marfan syndrome using high frequency ultrasound imaging.

***Hoxha B, College of Health Sciences, Midwestern University, Glendale, AZ , *Cameron E, Arizona College of Osteopathic Medicine, Midwestern University, Glendale, AZ ,** Talley NA, College of Health Sciences, Midwestern University, Glendale, AZ , Potter RM, College of Health Sciences, Midwestern University, Glendale, AZ , Vallejo-Elias J, Arizona College of Osteopathic Medicine, Midwestern University, Glendale, AZ , Esfandiarei M, College of Health Sciences, Midwestern University, Glendale, AZ , *These authors contributed equally to this work.

Marfan syndrome (MFS) is a systemic connective tissue disorder caused by mutations in the fibrillin-1 gene leading to various complications in multiple organs. However, aortic aneurysm is considered as the most life-threatening complications that may lead to aortic dissection, rupture, and sudden death. Previous studies have shown that transforming growth factor β (TGF-β) and angiotensin II type 1 receptor (ATII/AT1R) signaling play important roles during the progression of MFS aneurysm. Interestingly, both pathways are shown to be regulated by caveolin-1 (Cav-1), a structural protein within caveolae, which is highly expressed in vascular smooth muscle and endothelial cells. Studies in Cav-1 knock-out mice have reported that Cav-1 is required for normal ATII/AT1R signalling, while having inhibitory effects on TGF-β signaling and endothelial nitric oxide (eNOS) activity. Considering the complexity of CAV-1 regulatory function, we propose to investigate the effects of Cav-1 disruption by the cholesterol depleting agent methyl-β-cyclodextrin (MβCD) on the progression of aortic aneurysm in a mouse model of MFS. , Four weeks old MFS (Fbn1C1039G/+) and control mice received intra-peritoneal injection of MβCD (500mg/kg) twice a week, and cardiac and aortic structure and function was measured at 3 months of age using Vevo 2100 high resolution ultra sound imaging system (FUJIFILM VisualSonics). Measurements for aortic annulus, sinus of Valsalva and sinotubular junction diameters showed no difference between treatment and no treatment groups. Pulse wave velocity (PWV), which is an indication of aortic wall stiffness, was increased in MFS groups with a significant difference observed between MFS and control mice treated with MβCD. The dimensions

of the left ventricle were also evaluated by the measurements of interventricular septum in systole and diastole. Cardiac function was evaluated measuring the cardiac output, stroke volume, ejection fraction, early (E), and atrial (A) ventricular filling velocities, and E/A ratio, which showed no difference in MFS and control mice. Interestingly MβCD reduced mitral valve atrial velocity in both MFS and control groups. Using the tail-cuff method we also measured the blood pressure of these animals. The measurements showed no difference in the systolic and diastolic values of MFS and wild type treated with sham or MβCD. , This study although in an early stage has provided valuable information about the potential effects of Cav-1 manipulation by MβCD on cardiac and aortic function and structure in the mouse model of MFS associated aortic aneurysm.

Funding: Midwestern University

F11. Quantifying the Balance and Stability of a Powered Ankle-Foot Prosthesis using a Bio-Inspired Controller

***Huck TG, Northern Arizona University, Flagstaff, AZ ,** Hessel AL, Northern Arizona University, Flagstaff, AZ , Tahir U, Northern Arizona University, Flagstaff, AZ , Lockwood E, Northern Arizona University, Flagstaff, AZ , Petak J, Northern Arizona University, Flagstaff, AZ , Tester J, Northern Arizona University, Flagstaff, AZ , Nishikawa KC, Northern Arizona University, Flagstaff, AZ

Advances in prosthetic development have been driven largely by technology (e.g., light-weight materials, long-life batteries, and wireless communication), rather than by advances in our understanding of the underlying biological principles of movement. For a person with a transtibial (below the knee) amputation, the BiOM is a powered, ankle-foot prosthesis that utilizes a motor to assist the user through powered plantarflexion during stance and dorsiflexion during swing. The BiOM controller estimates the phase of the gait cycle and applies equations, optimized specifically for level walking, to command torque at the ankle joint. This permits faster preferred walking speeds than those produced using passive prostheses. However, this control approach exhibits no inherent adaptation to varying environmental conditions (i.e., stairs, slopes, and uneven ground), which is a notable quality of life and safety concern. Therefore, robust control algorithms that can perform well across a range of intended activities and variations of terrain, are needed. We developed a bio-inspired control algorithm for the BiOM based on a novel hypothesis for muscle contraction, the winding filament hypothesis (WFH). The WFH builds on the sliding filament theory by incorporating a role for titin, thus providing an explanation for intrinsic muscle properties previously unexplained by the sliding filament theory. In previous work, we demonstrated that the BiOM prosthesis implemented with a control algorithm based on the WFH not only produces ankle torque profiles during level walking at variable speeds that closely match the BiOM stock controller, but also produces ankle torque profiles similar to those of able-bodied individuals over variable terrain (grass and gravel) and during stair ascent. Our next step is to evaluate the balance and stability of individuals using the BiOM prosthesis with the WFH inspired control algorithm. This will be performed by analyzing whole-body angular momentum during walking on level, incline, and decline surfaces. Because whole-body angular momentum is a reliable measurement for quantifying fall risk, we will use this analysis to gain insights into the overall safety of the BiOM prosthesis with a WFH inspired control algorithm compared to the BiOM's stock controller and passive alternatives.

Funding: NSF (IIP-1237878 and IIP-1521231)

F12. OBESE VERSUS NON OBESE PATIENTS WITH SEVERE LOW BACK PAIN DURING GAIT

***Kuang K, University of Arizona, Tucson , AZ ,** Alejo G, University of Arizona, Tucson , AZ , Follis S, University of Arizona, Tucson , AZ , Wang J, University of Arizona, Tucson , AZ , Dohm M, University of Arizona, Tucson , AZ

Obesity and low back pain (LBP) are prevalent health issues that negatively affect ambulatory functions. Many studies have investigated the effects of LBP on gait; however, the effect of obesity remains largely unknown in

this population. The purpose of this study was to evaluate changes in gait parameters between obese and non-obese patients with severe LBP. We hypothesized that obese patients with LBP would display shorter stride length, higher cadence, and slower velocity compared to non-obese patients with LBP. Forty-four patients with LBP were included: 13 obese (7 males, 6 females; weight 94.41 ± 8.35 kg, height 1.64± .085 m, BMI 35.22±4.16 kg/ m2; age 58.54±14.44 years) and 31 non-obese (11 males, 20 females, weight 73.46±11.03 kg ; height 1.74±0.10 m; BMI 24.28±2.7 kg/ m2; age 55.74 ±11.06 years). The participants wore 5 inertial sensors (LEGSys™, Biosensics LLC, Cambridge, MA, USA) attached via elastic straps to their shins, thighs, and waist and were instructed to walk about 20 steps at their preferred pace. To investigate the effect of obesity, the Hotelling t-squared test was performed. Univariate independent t-tests were used when a main effect of the Hotelling test was significant. The level of statistical significance for all tests was set at $\alpha < 0.05$. The Hotelling test revealed a significant main effect of obese vs. non-obese groups ($p = 0.039$). We found that obese patients had increased stride time, double support, and coefficient of variation (CoV) of stride time (gait variability) (1.34±0.45 s, 28.66±12.07 %, and 5.56±2.82, respectively) compared to non-obese patients (1.13±0.09 s, 22.30±5.10 %, and 3.49±1.5, respectively). Of these differences, CoV was significant with a p-value of .002. Furthermore, obese patients had decreased stride length, stride velocity, and cadence compared to non-obese patients (1.00± 0.25 s vs. 1.17±0.21s, 0.81±0.26 m/s vs.1.04±0.24 m/s, and 94.80±17.09 steps/min vs. 106.85±8.72 steps/min) and all were significant with p-values of 0.011, 0.050, and 0.029, respectively. Our hypothesis is nearly supported as the obese patients showed slower stride velocity and shorter stride length, suggesting decreased gait function as compared to non-obese patients. Interestingly, for the obese group, the frequency of steps decreased as shorter stride length also decreased, underscoring the reduced stride velocity. Moreover, increased stride-to-stride variability (coefficient of variation of stride time) was also found for the obese group. Taken together, these results suggest that obese patients may be a unique population who require additional considerations when creating treatment plans for LBP.

F13. Role of Angiotensin II in Cardiovascular Stress Responses in Rats Exposed to Glucocorticoids In Utero

Madhavpeddi L, University of Arizona, Phoenix, AZ , Royal CR, University of Arizona, Phoenix, AZ , Hammond BD, Colorado State University, Fort Collins, CO , Handa, RJ, University of Arizona, Phoenix, AZ, Colorado State University, Fort Collins, CO , Hale TM, University of Arizona, Phoenix, AZ

It is well known that even transient prenatal insults can impact cardiovascular function in adulthood. We have hypothesized that adult cardiovascular disease may have its origins in utero as a result of exposure to elevated levels of glucocorticoids. In support of this, we have shown that when pregnant rat dams are treated with the glucocorticoid, dexamethasone (DEX), for the last 4 days of gestation, female-specific changes resulting in autonomic dysfunction and enhanced pressor and tachycardic responses to stress are detected in their adult offspring. Given the known role of angiotensin II in influencing the autonomic nervous system, the present study investigated the impact of antiogensin receptor antagonism on the cardiovascular stress responses in adult female rats that were exposed to DEX in utero. Pregnant dams were administered DEX (0.4mg/kg per day, s.c.) or vehicle on gestation days 18-21. This resulted in a significant reduction in birthweight in DEX-exposed males and females. At 2-3months of age, arterial pressure was assessed via radiotelemetry. In order to assess whether prenatal DEX alters stress-induced hypertensive and tachycardic responses, rats were placed in a restraint tube for 20 minutes, followed by a 2hr recovery period. Restraint-stress testing was performed on diestrus in females. Restraint stress was then repeated following a 5-day treatment with the angiotensin type 1 receptor antagonist, losartan (30mg/kg per day, i.p). Relative to vehicle-exposed rats, prenatal exposure to DEX resulted in enhanced elevations in systolic and diastolic pressure as well as heart rate in response to restraint stress. Treatment with losartan reduced the pressor and tachycardic responses to restraint, only in rats that were prenatally exposed to DEX. These findings suggest that prenatal programming of cardiovascular disease due to exposure to glucocorticoids may be mediated in part due to long-term changes in the renin angiotensin system.

Funding: ABRC ADHS14-082990

F14. Comparison of High-Nitrate versus Low-Nitrate Diets on Cardiovascular Health in Post-Menopausal Women

***Mayra SM, Arizona State University, Phoenix, AZ ,** Mayol-Kreiser, S, Arizona State University, Phoenix, AZ , Johnston, CS, Arizona State University, Phoenix, AZ , Sweazea, KL, Arizona State University, Tempe, AZ

This randomized, placebo-controlled, crossover trial compared the effects of fresh, high-nitrate vegetable salads (~ 445 mg nitrates/day) to canned, low-nitrate canned vegetables (~ <50 mg nitrates/day) on plasma nitrate/nitrite concentration, endothelial function, peripheral and central-aortic blood pressure, and arterial stiffness in a sample of post-menopausal. , Otherwise healthy, post-menopausal women (n = 5; 80% Caucasian; 52.6 ± 5.7 years) with mildly elevated blood pressure (mean blood pressure ≥ 115/70 mm Hg and < 140/80 mm Hg) were randomly assigned to ingest a fresh, high-nitrate vegetable salad (romaine lettuce, spinach, and celery) twice per day, for 10 consecutive days or a canned, low-nitrate vegetable medley (corn, green peas, and green beans) twice per day, for an equal duration of time. Pre- and post-condition measurements were obtained for all outcome variables, and participants completed a two to three week washout period followed by reassignment to the opposite condition. , Plasma nitrate/nitrite concentration was measured using a commercially available kit, peripheral blood pressure, central-aortic blood pressure, and arterial stiffness (measured by pulse wave velocity) were obtained via the non-invasive SphygomoCor XCEL system, and endothelial function (measured by flow-mediated dilation of the brachial artery) was obtained via a resolution 2D and doppler ultrasound with a linear-array transducer device. Wilcoxon signed-rank tests compared mean differences between conditions, and findings were considered significant at a p-value < 0.05. , Plasma nitrate/nitrite concentration was significantly higher following consumption of the high- versus the low-nitrate condition ($p = 0.043$), and flow-mediated dilation tended to increase following the high- versus the low-nitrate condition ($p = 0.080$). Conversely, differences in peripheral blood pressure were not statistically significant ($p = 0.345$ and $p = 0.684$ for systolic and diastolic pressure, respectively) nor were differences in central-aortic blood pressure statistically significant ($p = 0.225$ and $p = 0.465$ for systolic and diastolic pressure, respectively). Finally, there were no statistically significant differences in pulse wave velocity following the high- versus the low-nitrate condition ($p = 0.465$). , In conclusion, twice daily consumption of a fresh, high-nitrate vegetable salad significantly increased plasma nitrate/nitrite concentration, and while the trial was underpowered, there was a trend for improved flow-mediated dilation in this sample.

Funding: ASU: GPSA JumpStart Grant , Walmart , Safeway , Sprouts Farmers Market

F15. Impact of Bradykinin B1 Receptor Blockade on Angiotensin II-Induced Cardiac and Aortic Remodeling

***McCormick BA, University of Arizona College of Medicine -- Phoenix, Phoenix, AZ ,** Huot-Marchand J-E, University of Montreal, Montreal, Quebec, Canada , deBlois D, University of Montreal, Montreal, Quebec, Canada , Hale TM, University of Arizona College of Medicine -- Phoenix, Phoenix, AZ

Angiotensin II (AngII) is a growth factor known to induce vascular and cardiac hypertrophy and fibrosis. AngII has been shown to regulate bradykinin B1 receptor (B1R) expression in the heart and aorta and we have recently shown that concomitant B1R antagonism could prevent AngII-induced cardiac fibrosis. The present study investigated the impact of AngII and bradykinin B1R antagonism on blood pressure and left ventricular (LV) and aortic hypertrophy. Male Sprague-Dawley rats were treated for 4 weeks with vehicle or AngII (200 ng/kg per min) in the presence or absence of the B1R antagonist R-954 (400 µg/kg per day). In addition, bromodeoxyuridine (BrdU) was infused to assess cellular proliferation. At sacrifice, mean arterial pressure (MAP) was assessed via carotid artery cannulation in anesthetized rats. The LV and aorta were weighed, and the aortic and cardiomyocyte cross sectional area (CSA) were measured. Additionally, LV DNA content was determined and aortic cellular proliferation was assessed via immunohistochemistry to measure BrdU incorporation and ED-1 expression. Relative to vehicle, AngII increased MAP (59%), aortic cell proliferation (144%), and aortic CSA (34%), - effects that

were not offset by B1R antagonism. However, B1R antagonism did attenuate the AngII-induced increase in aortic mass. Similarly, AngII increased LV hypertrophy (35%) and total DNA content (44%) relative to control, both of which were prevented by concomitant B1R antagonism. Cardiomyocyte CSA was not different across treatment groups. AngII tended to increase macrophage density in the LV, and this was significantly reduced by concomitant B1R antagonism. This study reveals tissue-specific effects of bradykinin B1R antagonism. Although AngII induced significant remodeling in both the heart and aorta, concomitant B1R blockade only prevented cell accumulation, inflammation, and remodeling in the LV. Future studies will investigate the mechanism underlying this effect to further elucidate the role of the bradykinin B1R and its interaction with AngII in remodeling heart and aorta.

Funding: Canadian Male Sexual Health Council

F16. IMPAIRED SATELLITE CELL DIFFERENTIATION AND REGULATION IN LAMBS WITH INTRAUTERINE GROWTH RESTRICTION

Pendleton AL, University of Arizona, Tucson, AZ , Smith RM, University of Arizona, Tucson, AZ , Allen RE, University of Arizona, Tucson, AZ , Limesand SW, University of Arizona, Tucson, AZ

Establishing adequate muscle mass during fetal development is essential for viability and long term metabolic health. Fetuses subjected to conditions resulting in intrauterine growth restriction (IUGR) are born with less muscle mass than appropriate for gestational age infants, and never fully recover. Consequently, these individuals have an increased risk of developing a variety of metabolic syndromes, including Type 2 diabetes. To better understand the in-utero programming of IUGR on skeletal muscle growth and metabolism, we isolated satellite cells from one-month-old lambs. Here, we established a differentiation protocol showing increased differentiation of normal satellite cells grown on Matrigel compared to a fibronectin matrix, and this differentiation was exacerbated by the TGFβ inhibitor, A83-01. Through the development of the differentiation protocol, we found that the differentiation of IUGR satellite cells was greater than control satellite cells. However, the difference between IUGR and control satellite cell differentiation rates was negated when both cultures were exposed to A83-01. Moreover, our findings show differential regulation of SMAD4, a key component of TGFβ signaling, between normal and IUGR satellite cells. Specifically, IUGR satellite cells exhibit altered SMAD4 nuclear translocation events evidenced by modification of the protein. Together, these findings demonstrate for the first time that satellite cells from IUGR lambs exhibit altered differentiation capacity indicating satellite cell programming is influenced by conditions associated with IUGR.

Funding: R01 5R01DK084842-07

F17. Impact of Prior ACE Inhibition on Cardiac Fibroblast Physiology

***Perez O, University of Arizona, Phoenix, AZ ,** Hale TM, University of Arizona, Phoenix, AZ

Transient angiotensin converting enzyme (ACE) inhibition induces persistent changes that protect against future fibrosis, fibroblast proliferation, and macrophage infiltration in response to injury. Moreover, fibroblasts isolated from injured hearts of rats that were previously treated with an ACE inhibitor proliferate at a slower rate than those isolated from injured hearts of naïve rats. ACE inhibitors have also been shown to produce apoptosis of 30% of cardiac fibroblasts in adult spontaneously hypertensive rats (SHR). It may be that the long-term protection afforded by transient ACE inhibition is due to apoptosis of a sub-population of pathological fibroblasts. The present study investigates whether cardiac fibroblasts isolated from SHR previously treated with an ACE inhibitor display different proliferative properties than those isolated from control SHR. We evaluated changes in cardiac mass and DNA content in the left ventricles of adult male SHR previously treated for 2 weeks with the ACE inhibitor enalapril (30mg/kg per day, p.o.) followed by a 2-week washout period. In separate rats that underwent the same treatment protocol, cardiac fibroblast were isolated and cultured to P1 to evaluate differences in basal

proliferation rates. SHR previously treated with the ACE inhibitor followed by a 2-week washout period showed a 10% ($p<0.05$) reduction in left ventricular mass, compared to untreated control. This was accompanied by a 12% ($p<0.05$) reduction in left ventricular DNA content. However, population doubling assessments did not reveal significant differences in the proliferation rates of fibroblasts isolated from control rats, compared to those isolated from SHR previously treated with enalapril. Given that ACE inhibition has been shown to induce apoptosis exclusively in fibroblasts, the persistent reduction in DNA content suggests that there may be a sustained reduction in fibroblast content. Although we have previously demonstrated that fibroblasts from previously treated rats proliferate more slowly in response to cardiac injury, the present data suggests that under basal conditions, the cells are not hypoproliferative. Future studies will investigate whether fibroblasts from ACE inhibitor-treated rats program to different phenotypes in response to a pathological stimulus.

Funding: College of Medicine – Phoenix Springboard grant

F18. Noradrenergic and cholinergic modulation of Dbx1 XII inspiratory premotoneurons

Revill AL, Midwestern University, Glendale, AZ , Funk GD, University of Alberta, Edmonton, AB

Sleep specific reductions in the tonic and inspiratory activity of XII motoneurons that innervate the genioglossus muscle of the tongue, the main tongue protruder, are causally implicated in obstructive sleep apnea. This decreased activity is hypothesized to result from reductions in both glutamatergic inspiratory drive and excitatory modulation. Inspiratory drive to XII motoneurons is generated by the preBötzinger Complex (preBötC) and transmitted via inspiratory XII premotoneurons. preBötC drive is minimally affected by sleep state, but little is known of the sleep-dependent modulation of XII inspiratory premotoneurons, except that in carbachol-induced rapid eye movement-like sleep, inspiratory XII premotoneuron activity decreases. Regardless of changes in XII motoneuron excitability, XII inspiratory output will cease in sleep if the premotoneurons fall silent. Thus, our objective is to determine the effects of neuromodulators whose levels change with sleep (e.g., noradrenaline and acetylcholine) on the excitability of Dbx1-derived XII inspiratory premotoneurons in the intermediate reticular formation (IRt). , , We generated rhythmic, transverse medullary slices (550-600 μm) from Dbx1Cre; R26tdTomato neonatal mice (postnatal day 1-5), identified inspiratory, Dbx1-derived IRt premotoneurons using whole-cell recording, locally applied phenylephrine (100 μM, α1 noradrenergic agonist) and muscarine (100 μM, muscarinic acetylcholine agonist) and assessed effects on membrane and synaptic properties. Preliminary data (n=10) indicate that phenylephrine depolarized membrane potential and increased both inspiratory and evoked spiking activity. Furthermore, phenylephrine induced inward currents that were associated with modest 15-20% increases in input resistance, but had minimal effect on inspiratory synaptic currents. Muscarinic receptor activation (n=4) had small, variable effects on inspiratory and membrane currents, and on input resistance. Preliminary data suggest that excitability of Dbx1-derived, XII inspiratory premotoneurons is sensitive to noradrenergic excitation and cholinergic inhibition. Thus, during sleep, if noradrenergic tone falls and cholinergic tone increases in the IRt as in the XII nucleus, these changes may contribute to the state-dependent reduction in airway muscle tone implicated in sleep-disordered breathing. Funding: CIHR, WCHRI, AIHS, CFI

Funding: Canadian Institutes of Health Research , Women and Children's Health Research Institute , Alberta Innovates Health Solutions , Canadian Foundation for Innovation

F19. Ultrasonic vocalization and physiological responses in rats

Ann Marie Wronkowski, Midwestern University, Glendale, Az, Maverick Lasker, Arizona State University, Tempe, AZ, Tobias Riede, Midwestern University, Glendale, Az

Vocal communication is one of the most complex behaviors in both humans and animals. It requires muscle control to drive breathing, adjust laryngeal configuration and move tongue and jaw. The goal of this project was

to investigate the effect of changes to the autonomic nervous system (ANS) on the vocal sound output. If changes to the ANS are reflected in the vocal output, an animal's vocalization could serve as non-invasive tool to better understand wellbeing. The ANS could affect vocalization either directly by acting on all three motor systems involved, or by affecting the emotional state of the animal and modulatory effects on the hindbrain. Work in nonhuman primates and rodents suggests a strong relationship between ANS activation and call rates. However, those studies have been performed in juveniles. The role of the ANS in adult animals has remained unclear. We used heart rate (HR) to estimate ANS activation and tested the hypothesis that vocal characteristics are associated with sympathetic activation in rats (Rattus norvegicus). If changes in the ANS activation are reflected in the vocal output, we expected that acoustic features, such as fundamental frequency, call duration and sound intensity, would co-vary with HR. Preliminary data suggest that average HR is elevated at call onset but often decreases quickly back to baseline, although the rat continues to call. Fundamental frequency does not co-vary in a consistent pattern. Interestingly, in all animals tested, HR variation was significantly higher during vocalization than during baseline recording. If HR variation is related to the emotional responding of an animal, as suggested by other researchers, vocalization could serve as a noninvasive proxy.

F20. Feasibility of MRI-RHC based pressure volume loops in control and PAH patients

Rosado-Toro JA, University of Arizona, Tucson, AZ , Avery RJ, University of Arizona, Tucson, AZ , Altbach MI, University of Arizona, Tucson, AZ , Rischard F, University of Arizona, Tucson, AZ , Vanderpool RR, University of Arizona, Tucson, AZ

Right ventricular (RV) function is a major determinate of mortality in patients with pulmonary arterial hypertension (PAH). RV coupling obtained from full conductance derived pressure-volume (PV) loops are difficult to obtain in clinical settings. Thus, simplified methods have been introduced but are limited as they rely on end-diastolic (ED) and end-systolic (ES) volumes. Presented is a novel method to measure full PV loops using cardiac magnetic resonance (CMR) images to generate volumetric data. We hypothesize that it is feasible to generate full clinical PV loops from CMR images to more accurately measure RV coupling than simplified methods. , PV loops were generated in 9 subjects (5 control, 4 PAH) who had a CMR exam and right heart catheterization (RHC) within 48 hours. RV volumes were derived by propagating manually traced RV endocardium in the ED and ES frames throughout the cardiac cycle using an automated dynamic programming technique (Fig. 1A). RV volumes were matched with RHC-measured RV pressure using linear interpolation. Treatment naïve patients underwent repeat RHC/CMR following the initiation of parenteral treprostinil. , PAH patients demonstrated increased mean pulmonary arterial pressure (mPAP) (57 ± 10 mmHg vs 20 ± 5 mmHg) and decreased RV ejection fraction (RVEF) (26 ± 11% vs 55 ± 4%) when compared to controls. Representative PV loops for a control and a moderate PAH (middle) and severe PAH (right) demonstrate the late-systolic increase in RV pressure, previously observed using conductance catheters (Fig. 1B). The response to treprostinil therapy (Figs. 1C-D) consisted of a decrease in mPAP, an increase in RVEF and a patient-specific change in RV volumes. ES and ED volumes decreased in (Fig. 1C) but only the ES volume decrease in (Fig. 1D). , Full RV PV loops obtained by our CMR-RHC method show the contour is significantly altered in PAH; this is not easily estimated using the simplified rectangular PV loop approach.

Funding: T32-HL007955, HL085385

F21. Accumulation of Gut Bacteria May Cause the Age-Related Decline of Anoxia Tolerance in Adult Drosophila melanogaster

Sargent JC, Arizona State University, Tempe, AZ , Campbell JB, Arizona State University, Tempe, AZ, Harrison JF, Arizona State University, Tempe, AZ

Cell death occurring from anoxia is the major pathology during heart attack, stroke and multiple other diseases. Humans vary substantially in their ability to survive anoxia, especially across ages, and the basis to this variation is

not well-understood. Drosophila melanogaster have similar metabolic pathways to humans but have much better capacities to tolerate anoxia, suggesting that understanding mechanisms of anoxia tolerance in flies may provide insight for the development of new medical treatments. We exposed adult Drosophila, ages 1, 3, 5, 7, 9, and 12 days old, to six hours of anoxia and assessed survival 24-hours post-treatment. Seventy-nine percent of adults one day past eclosion survived; while only 10% of twelve-day-old adults survived; thus Drosophila show age-related decline in anoxia tolerance like humans. In anoxia, ATP levels declined rapidly (< 30 min) to near-zero levels in both 1 and 12 day old adults; thus the better anoxia-tolerance of young adults is not due to a better capacity to maintain cellular energetic status. The concentration of bacteria in the gut is known to increase strongly with age in Drosophila. To test whether declining anoxia tolerance might be due to this increasing bacterial load, we replaced their food daily, every third day, or every sixth day, allowing us to vary gut bacterial load from low to high, respectively. At 12 days of age, each treatment group was exposed to six hours of anoxia and assayed for gut bacterial load. Anoxia tolerance was strongly and negatively affected by bacterial load. These data suggest that increasing bacterial load may play an important role in the age-related decline of anoxia tolerance in Drosophila, perhaps because anoxia enhances the capacity of bacteria to penetrate the gut and infect the organism. This research was supported by NSF IOS 1256745 and support from the SOLUR program of the School of Life Sciences.

Funding: NSF IOS 1256745 and support from the SOLUR program of the School of Life Sciences

F22. Differential sphingosine-1-phosphate receptor 1 expression following middle cerebral artery occlusion in murine heart and brain

***Shi S, University of Arizona, Phoenix, AZ ,** Mohamed A, University of Arizona, Phoenix, AZ , Rodriquez J, University of Arizona, Phoenix, AZ , Liu, Q, Barrow Neurological Institute, Phoenix, AZ , Gonzales, R, University of Arizona, Phoenix, AZ

Stroke is a leading cause of death in the US and is a major cause of serious disability. Pathophysiologically, ischemic brain injury can trigger an inflammatory response leading to disruption of the blood brain barrier promoting brain-infiltrating immune cells which can contribute further to the release of inflammatory factors. We and others demonstrate that “nonselective” sphingosine-1 phosphate receptor (S1PR) modulators provides neuroprotection during stroke. However, despite these effective outcomes, nonselective actions of S1PR modulators have been shown to elicit undesired off target effects such as bradycardia as a result of high affinity binding to multiple S1PR subtypes. Identifying more selective S1PR modulators with neuroprotective potential will reveal better drug development for treatment of ischemic stroke especially for patients with co-morbidities such as cardiovascular disease. S1PR is a G-protein-coupled receptor that is expressed in a number of organ systems, including the in immune and cardiovascular systems. Recently, we have shown preclinical evidence that selective S1PR type 1 (S1PR1) modulation can reduce parenchymal damage via attenuation of peripheral nodal egress. However, the role of S1PR1 in the brain, especially following stroke remains to be investigated. Here we investigated whether selective S1PR1 is expressed in the brain and heart, and whether S1PR1 levels are altered after ischemic injury. Adult female mice were subjected to 60-min transient middle cerebral artery occlusion (MCAO). Post 24 h reperfusion animals were perfused with ice cold PSS and whole brain and heart removed. The brain was divided into ipsilateral (stroke side) and contralateral hemispheres. Both heart and brain were homogenized and analyzed for total protein. Immunoblotting was performed for S1PR1 receptor expression in sham vs. MCAO. We observed that S1PR1 is expressed in both brain and heart under non-pathophysiological conditions. Following ischemic injury, S1PR1 brain expression increased compared to sham. Specifically, S1PR1 protein levels were greater in the ipsilateral compared contralateral side. Conversely, in the heart, S1PR1 protein levels were decreased in MCAO injured animals compared to sham. In conclusion, selective S1PR1 modulation may be a significant therapeutic target for treatment of ischemic stroke since expression increases in the brain and decreases in the heart, an organ with adverse effects following nonselective S1PR modulation. Future studies

will investigate the beneficial effect of selective S1PR1 modulation in the brain on mechanisms associated with protective neurological outcome during ischemic injury.

Funding: Valley Research Partnership P2 (RG)

F23. Role of Inducible Nitric Oxide Synthase (iNOS) in Marfan Syndrome Associated Aortic Aneurysm

Talley NA, College of Health Sciences, Midwestern University, Glendale, AZ , Hoxha B, College of Health Sciences, Midwestern University, Glendale, AZ , Alexander T, College of Health Sciences, Midwestern University, Glendale, AZ , Cameron, E, Arizona Colllege of Osteopathic Medicine, Midwestern University, Glendale, Az , Gibson C, Arizona College of Osteopathic Medicine, Midwestern University, Glendale, AZ , Vallejo-Elias J, Arizona College of Osteopathic Medicine, Midwestern University, Glendale, AZ , Esfandiarei M, College of Health Sciences, Midwestern University, Glendale, AZ

Marfan syndrome (MFS) is an autosomal dominant inherited disease that effects the connective tissue of large vessels throughout the human body. MFS is caused by a mutation in the FBN1 gene which encodes for fibrillin-1, a major component of extracellular microfibrils and acts as a scaffolding protein for elastin deposition and allows for the formation of elastic fibers in the extracellular matrix of large arteries. The loss of aortic wall structural integrity leads to the cardiovascular manifestations of MFS, which include the dilation of the aortic root that can lead to thoracic aortic root dissection and rupture. Previous studies have shown that the activity of endothelial nitric oxide (eNOS) has decreased in the aortic wall leading to endothelial dysfunction in MFS mice. However, we have been able to show that despite an obvious decrease in eNOS activity, the basal NO level in the aortic tissue is significantly higher in MFS mice aorta. This observation suggests that other isoforms of NOS may also play roles during MFS aneurysm progression. In this study, we hope to determine the role that inducible nitric oxide synthase (iNOS) may play in MFS aneurysm pathogenesis by creating a MFS mouse lacking iNOS expression. MFS (FBN +/-) and MFS mice lacking iNOS expression (FBN+/-, iNOS-/-) were subjected to high resolution high frequency ultrasound imaging at the age of 3 months to evaluate cardiac and aortic structure and function. Our data shows that the dimensions of the Sinus of Valsalva were greater in MFS mice when compared to control mice and mice lacking iNOS expression. Pulse wave velocity is greater in MFS and MFS/iNOS KO mice compared to control, which is the indication of increased stiffness of the aortic wall in these groups as compared to control aorta. Additionally, cardiac output, ejection fraction, stroke volume, fractional shortening, early (E), and atrial (A) ventricular filling velocities were evaluated and E/A ratio showed significant differences between the mice lacking the iNOS expression and MFS mice. This study although in an early stage provides valuable information about the potential effects of iNOS manipulation on cardiac and aortic function and structure in the mouse model of MFS associated aortic aneurysm.

Funding: Midwestern University, College of Health Sciences

F24. 3D scanning of a human body for dimensional measurements and detection of changes

***Weimer E, Grand Canyon University, Phoenix, AZ , *Hoskins K, Grand Canyon University, Phoenix, AZ,** Artzi I, Grand Canyon University, Phoenix, AZ

Purpose Statement: The feasibility of using an inexpensive 3D scanning system on a human body for dimensional measurements and subsequent detection of changes. Materials/Methods: The materials used included a 3D StructureSensor, an iPad, laptop, Skanect software, and a mannequin. Our method makes an innovative use of 3D scanning and subsequent processing of captured data. First, we created 3D geometrical representations of body segments. Then we developed a mathematical model for representing the body segments. We also developed an algorithm which searches for those patterns within the dataset of body segments generated by the full body scan. When a match is found in the dataset, it means that a body segment has been identified. Summary of Results: We

found an effective way of determining specific dimensions of a subject that was scanned. We developed a machine-learning based classifier software tool that categorizes human body segments after being presented with a large and diverse set of human bodies. The classifier implemented an adaptation of the k-means algorithm to automatically identify generic groups of subjects (body types). The resulting classification offered a reference framework for comparison with new scanned bodies. The high-resolution body scan enabled us to detect small differences between a scanned subject and the reference body segment. These differences can then be mapped onto known symptoms of various health problems, typically manifested as slight deformations of various body segments. Conclusion: Our approach shows promise in the identification of changes for multiple locations on the human body simply by performing a 3D scan of the subject, with a consistent and quantifiable degree of accuracy.

Funding: Grand Canyon University, Self-funded

F25. Reduced skeletal muscle transcription factor expression response to exercise in insulin resistance

***Zapata-Bustos R, University of Arizona, Tucson, AZ ,** Finlayson J, University of Arizona, Tucson, AZ , De Filippis E, Mayo Clinic, Scottsdale, AZ , Mandarino LJ, University of Arizona, Tucson, AZ

Previous studies show lower PPARγ coactivator PGC-1α expression in muscle of insulin resistant subjects. Lower PGC-1α can lead to changes in mitochondrial protein abundance and bioenergetic changes that lead to an altered response to exercise. Although there is evidence of abnormal gene expression responses to exercise in insulin resistance, it is not known if there is an underlying, coordinated lower exercise response of transcription factors. Preliminary data identified several transcription factors (EGR1, KLF4, SP1 and NFKB1) as possible regulators of exercise-induced gene expression responses in healthy subjects. The purpose of this study was to determine whether these and other transcription factors have reduced responses to exercise in obese, insulin resistant subjects. Insulin sensitivity of 6 lean and 6 obese subjects was assessed using a euglycemic hyperinsulinemic clamp. Muscle biopsies of the vastus lateralis were taken in resting conditions, 30 minutes and 24 hours after a single 48 min bout of exercise. Quantitative RT-PCR was used to determine the effect of exercise on gene expression. Obese subjects were insulin resistant (glucose disposal rate of 11.84±0.81 mg/kg-1·min-1 vs 5.32±1.18 mg/kg-1·min-1, lean vs obese). Analysis of mRNA for EGR1, EGR2, EGR3 and KLF4 showed that compared to resting conditions (set to 1.0) there was a significant increase in gene expression after 30 min of exercise in the lean controls (12.07±10.23, 2.5±1.15, 4.14±1.3 and 9.16±3.82, respectively). After 24 hrs. post exercise, expression of EGRs and KLF4 decreased to resting levels. On the other hand, the obese group, compared to lean control values of 1.0, had lower basal mRNA for EGR1 (0.22±0.06), EGR2 (0.23±0.11), EGR3 (0.32±0.07) and KLF4 (0.77±0.21), and had reduced response to exercise at 30 min, compared to lean controls (1.39±0.683, 0.32±0.11, 0.98±0.41 and 0.76±0.11, respectively). The lower response in the transcriptional program suggests that the obese insulin resistant group is also exercise resistant when compared to the insulin sensitive lean control group. The blunted transcriptional program to exercise could explain the lower subsequent resting protein abundance and mRNA levels previously documented in insulin resistance.

Funding: NIH-R01DK47936 , NIH-R01DK66483

SATURDAY PRESENTATIONS

S1. 3D scanning of a human body for dimensional measure*Erikments and detections of changes

***Weimer E, Grand Canyon University, Phoenix, AZ , *Hoskins K, Grand Canyon University, Phoenix, AZ ,** Artzi I, Grand Canyon University, Phoenix, AZ

Purpose Statement: The feasibility of using an inexpensive 3D scanning system on a human body for dimensional measurements and subsequent detection of changes. Materials/Methods: The materials used included a 3D StructureSensor, an iPad, laptop, Skanect software, and a mannequin. Our method makes an innovative use of 3D scanning and subsequent processing of captured data. First, we created 3D geometrical representations of body segments. Then we developed a mathematical model for representing the body segments. We also developed an algorithm which searches for those patterns within the dataset of body segments generated by the full body scan. When a match is found in the dataset, it means that a body segment has been identified. Summary of Results: We found an effective way of determining specific dimensions of a subject that was scanned. We developed a machine-learning based classifier software tool that categorizes human body segments after being presented with a large and diverse set of human bodies. The classifier implemented an adaptation of the k-means algorithm to automatically identify generic groups of subjects (body types). The resulting classification offered a reference framework for comparison with new scanned bodies. The high-resolution body scan enabled us to detect small differences between a scanned subject and the reference body segment. These differences can then be mapped onto known symptoms of various health problems, typically manifested as slight deformations of various body segments. Conclusion: Our approach shows promise in the identification of changes for multiple locations on the human body simply by performing a 3D scan of the subject, with a consistent and quantifiable degree of accuracy.

Funding: Grand Canyon University, - self-funded

S2. Relationship between animal class and dietary profile on blood glucose concentrations

***Basile AJ, Arizona State University, Tempe, AZ** , Caskey A, Arizona State University, Tempe, AZ , Jarrett C, Arizona State University, Tempe, AZ , Sweazea KL, Arizona State University, Tempe, AZ

Blood glucose serves as a circulating fuel source for animals, however, species vary in glucose requirements due to distinct fuel physiology. The goal of this study was to examine blood glucose levels across four classes within the animal kingdom: Amphibia (n = 6 species), Aves (n = 163 species), Mammalia (n = 121 species), and Reptilia (n = 85 species) as well as compare glucose levels by diet profile (herbivore, omnivore, insectivore, frugivore/nectarivore, carnivore, granivore, and piscivore) within and across animal class. Data on diet profile, fasting blood glucose levels, and body mass were obtained for 375 species of animals housed at The Phoenix Zoo in Arizona. Data were analyzed using one-way ANOVA with p-values of <0.05 considered statistically significant. Consistent with prior studies, Aves maintained the highest fasting plasma glucose levels among vertebrates. Within Aves, animals consuming either insectivorous or granivorous diets had the highest glucose concentrations. For insectivores, the high glucose concentrations are likely attributed to de novo gluconeogenesis. Likewise, within Reptilia insectivorous animals maintain the highest glucose concentrations. Data from captive animals is advantageous as the dietary profile and life history of each animal is known, thereby minimizing the unpredictability of wild life. The goal of this ongoing study is to better understand evolutionary variations in glucose regulation.

S3. Genistein-induced weight loss in ob/ob diabetic mice is associated with reductions in serum metabolic and cytokine markers

***Archana Chandrashekar,** Ryan Lord, Taylor Bowman and Layla Al-Nakkash

Obese diabetic ob/ob mice are hyperphagic, hyperinsulinemic and hyperglycemic, and thus mimic the clinical obese-diabetic state. The goal of this study was to determine whether dietary genistein (600 mg genistein/kg diet, 600G) would reduce the obese-diabetic phenotype of the ob/ob mouse. Genistein is a naturally occurring isoflavone found in soy. At age 5-6 weeks, ob/ob mice were maintained on one of the following diets for 4-weeks; standard rodent diet, or genistein diet (600G). We compared the diabetic-obese model to lean mice fed standard rodent diet. Body weight at the end of the diet study was 9% lower in males fed 600G and 13% lower in males fed 600G. Liver weight was unchanged by genistein diet. Total abdominal fat pat weight was significantly reduced ~1 g with genistein diet in female ob/ob mice. Genistein diet reduced serum glucose levels in females by 18% (from 476.7 ± 15.2 to 389.1 ± 39.7 mg/dL, n = 11, $P<0.05$) and in males by 43% (from 604.0 ± 56.2 to 345.8 ± 21.1 mg/dL, n = 7, $P<0.05$). There was no effect of genistein diet on insulin level. Serum triglyceride levels were 2.2-fold elevated in the ob/ob mice and genistein diet significantly reduced this to levels seen in leans. Serum levels of pancreatic polypeptide, PP, were significantly increased in females (from 6.75±1.29 to 33.22 ± 9.37 pg/ml, n = 6) and males (from 18.67±6.90 to 48.54±13.69 pg/ml, n = 6). Genistein diet induced a 56% rescue of PP in female ob/ob mice. Serum levels of peptide YY, were significantly increased in females (from 49.34±4.08 to 66.89±6.78 pg/ml, n = 6) and males (from 30.01±11.15 to 87.99±4.63 pg/ml, n = 6) and genistein diet was without effect. Serum glucagon levels were significantly increased 7-fold in female ob/ob mice and genistein diet had no effect. Serum glucose-dependent insulinotropic polypeptide, GIP, levels were comparable in both sexes of ob/ob mice verus lean counterparts and genistein diet significantly increased GIP levels in ob/ob females 2.3-fold (from 258.79±47.37 to 5584.21±73.14 pg/ml, n = 7, $P<0.05$). We conclude that feeding ob/ob mice genistein (600G) diet for 4-weeks; (1) induced weight loss in both females and males, (2) reduced serum glucose and triglyceride levels in females and males, (3) reduced serum PP levels in females, (4) increased serum GIP levels in females. These studies could have impact on clinical interventions to induce weight loss and reduce diabetic phenotype in the obese-diabetic population.

Funding: Archana Chandrashekar was supported by the MWU Summer DO Fellowship Program. Layla Al-Nakkash was supported by: Soy Health Research Program, Diabetes Action Research & Education Foundation and MWU Intramural funds.

S4. The function of the CD47 and NO/cGMP signaling in tumor progression

***Chung SI, University of Arizona, Tucson, AZ ,** Young SM, University of Arizona, Tucson, AZ , Lara HI, University of Arizona, Tucson, AZ , Schwenker AD, University of Arizona, Tucson, AZ , Montfort WR, University of Arizona, Tucson, AZ

CD47 is an immune checkpoint molecule that is overexpressed in cancer cells. It is a transmembrane protein and by binding signal regulatory protein alpha (SIRP α), a molecule expressed macrophages and dendritic cells, it inhibits phagocytosis and activation of CD8+ T cells. Blocking CD47/SIRP α interactions have resulted in anti-tumor effects, and an anti-CD47 antibody is currently under evaluation in a clinical trial for tumors. Research on CD47 has focused on the CD47/SIRP α interaction, however CD47 also binds matricellular protein thrombospondin-1 (TSP-1) and regulates various normal physiological functions. However, the function of CD47/TSp-1 signaling in the tumor microenvironment has not been well explored. In endothelial, smooth muscle, and platelet cells, CD47/TSP-1 interaction inhibits the NO-soluble guanylyl cyclase (sGC)-cGMP pathway, a pathway that regulates tumor promotion. We hypothesize that the CD47/TSP-1 signaling occurs in tumor and immune cells and that it is involved in tumor progression. To address our hypothesis, we will use normal human breast (MCF10a) and human breast cancer (MDA-MB-468) cells and OT-1 T-cells. These cells will be treated with

full-length TSP-1 or with C-terminal TSP-1 fragment, E3CaG1. Following treatment, the cells will be stimulated with DEA/NO, a NO donor, and cGMP levels will be assessed. To confirm that CD47 is necessary for TSP-1-driven inhibition of sGC activity, CD47 signaling will be blocked by knocking down CD47 and/or by using anti-CD47 antibody. Using the same treatment scheme, in vitro assays that measure tumor and immune cell phenotypes will be performed to determine if CD47/TSP-1 binding regulates tumor promotion. sGC activators will also be used to confirm that sGC is involved in the CD47/TSP-1 regulation of tumor progression. Presently, we have preliminary data showing that CD47 is expressed on MDA-MB-468 cells and that NO stimulates sGC activity in these cells. Interestingly, NO did not stimulate sGC activity in MCF10a cells due to a decrease in sGC expression. Treatment of MDA-MB-468 cells with 8-Br-cGMP, a hydrolysis-resistant analogue of cGMP, had no effect on tumor cell growth and motility. Based on our data, MDA-MB-468 expresses CD47, and NO can stimulate sGC activity in these cells suggesting that MDA-MB-468 cells is a valid cell model to study the role of CD47 and NO signaling in tumor cells. Our data suggests that the sGC pathway may not play a role in the cell growth and migration of MDA-MB-468 cells, however it may be involved in other tumor functions which is currently being investigated. Our work will further the understanding of CD47 and NO signaling function in tumor promotion.

Funding: T32 CARDIOVASCULAR RESEARCH PROGRAM, ORD Pilot Grant

S5. The lipidated connexin mimetic peptide, SRPTEKT-Hdc, is a potent inhibitor of Cx43-mediated intercellular communication with specificity for the pS368 phospho-form

***Cotter ML, University of Arizona, Tucson, AZ,** Boitano S, University of Arizona, Tucson, AZ, Vagner J, University of Arizona, Tucson, AZ, Burt JM, University of Arizona, Tucson, AZ

Connexin mimetic peptides derived from extracellular loop II sequences (e.g. Gap 27: SRPTEKTIFII, and Gap36: KRDPCHQVDCFLSRPTEK) have been used as reversible, Cx-specific blockers of gap junction intercellular communication (GJIC). These blockers typically require high concentrations (100-200 μM with IC50s of ~20-30 μM) to achieve inhibition. We have shown that addition of a hexadecyl (Hdc) lipid tail to the conserved SRPTEKT peptide sequence, SRPTEKT-Hdc, results in a novel, highly efficacious and potent GJIC inhibitor. Mechanically-induced Ca2+ wave propagation in Madin-Darby Canine Kidney cells expressing mCx43 (MDCK43) was significantly inhibited following a 60-90 min incubation in SRPTEKT-Hdc; IC50 of SRPTEKT-Hdc inhibition was 66.5 pM (95% CI: 31.8-138.9 pM). Lipidated reverse-sequence (TKETPRS-Hdc) and scrambled sequence (EPTKRTS-Hdc) peptides had no effect. SRPTEKT-Hdc also decreased NBD-m-TMA, but not Alexa350, dye coupling, but not to the same extent as inhibition of Ca2+ waves. Reduction of plaque-associated Cx43 (an indicator of channel number) in cells treated with SRPTEKT-Hdc could not explain the loss of Ca2+ wave propagation. However, we did find that SRPTEKT-Hdc inhibition of Ca2+ wave propagation depended on the functional configuration of Cx43 in which the S368 site is phosphorylated (pS368). Ca2+ wave propagation was enhanced in MDCK cells expressing single site mutants of Cx43 that favored or mimicked phosphorylation at S368 (MDCK43-S365A and MDCK43-S368D). Further, Ca2+ wave propagation in MDCK43-S365A and -S368D cells was inhibited by SRPTEKT-Hdc whereas Ca2+ wave propagation in MDCK43-S365D and -S368A cells, mutations that favor or mimic dephosphorylation at S368, was largely unaffected by SRPTEKT-Hdc. Together, these data indicate that SRPTEKT-Hdc is a potent inhibitor of physiologic Ca2+ wave signaling mediated specifically by the pS368 phospho-form of Cx43.

Funding: T32HL7249 , R01HL58732 , R01NS073664

S6. NOVEL ORGANOMETALLIC COMPLEX LOWERS NON-HDLc IN MALE ADOLESCENT RATS FOLLOWING 10-WEEK HIGH FAT DIET

***Crawford, M, Arizona State University, Tempe, AZ ,** Clark, W, Arizona State University, Tempe, AZ , Sweazea, KL, Arizona State University, Tempe, AZ

The prevalence of childhood obesity has increased substantially in the United States over the last decade. Obese children and adolescents are more likely to have hypercholesterolemia, which is a major risk factor for cardiovascular and metabolic disorders. The following study examined the metabolic effects of a soil-derived organometallic complex (OMC) on 6-week old periadolescent male Sprague Dawley rats. Rats were divided into two dietary groups: standard chow (18.9% protein, 57.33% carbohydrates, 5% fat) or a high-fat diet (HFD; (20% protein, 20% carbohydrates [6.8% sucrose], 60% fat) for 10 weeks. Rats were further divided and treated with OMC in their drinking water at one of the following doses: vehicle (0 mg/mL), 0.6 mg/mL or 3.0 mg/mL. HDL cholesterol significantly decreased in HFD fed rats at 6 weeks ($p=0.006$) and 10 weeks ($p=0.003$). Additionally, HDL cholesterol was not significantly altered in HFD rats treated with OMC. OMC-treated HFD rats had significantly lower non-HDLc (LDL and VLDL) levels after 6 weeks of both 0.6 mg/mL ($p<0.001$) and 3.0 mg/mL ($p=0.008$) OMC administration, with similar results at 10 weeks [0.6 mg/mL ($p=0.008$) and 3.0 mg/mL ($p=0.012$)]. These decreases in non-HDLc may prevent some of the metabolic dysfunctions associated with obesity and insulin resistance. Overall, these findings suggest that OMC may play a cardioprotective role in preventing metabolic syndrome in adolescent rats.

Funding: This study was funded by a grant from Isagenix International, LLC.

S7. Respiratory muscle training impacts daytime and overnight blood pressure in adults with obstructive sleep apnea

DeLucia, CM, University of Arizona, Tucson, AZ , Ramos Barrera GE, University of Arizona, Tucson, AZ , De Asis RM, University of Arizona, Tucson, AZ , Bailey EF, University of Arizona, Tucson, AZ

Inspiratory muscle training lowers blood pressure in healthy, college-aged individuals and adults with mild and moderate obstructive sleep apnea (Vranish & Bailey 2015; 2016). The mechanisms underlying respiratory training related reductions in blood pressure are unknown and it is not clear if individuals with more severe forms of sleep apnea can benefit from the intervention. Here, we explore the integrative physiological benefits of 6 weeks of daily respiratory training on sleep, blood pressure, and autonomic nervous system activity in adults with moderate-severe obstructive sleep apnea. All subjects (N=21) initially underwent in-home sleep studies and 24-hour blood pressure monitoring to determine sleep apnea severity. Subsequently, we recorded efferent sympathetic nerve traffic and assessed baroreflex sensitivity and daytime blood pressures. To date, 14 males and 7 females (66.74± 1.78 years; average AHI of 28.84 ± 3.81) have completed daily respiratory muscle or sham training over 6 weeks. We report declines in resting daytime (129.27± 5.18 mmHg vs. 119.45± 5.11 mmHg) and nighttime (118.25± 6.58 mmHg vs. 113.17± 3.70 mmHg) systolic blood pressures in the treatment group with no change in daytime (137.20± 3.80 mmHg vs. 135.40± 4.30 mmHg) or nighttime (139.8± 2.57 mmHg vs. 145.7± 3.21 mmHg) systolic pressures in sham trained subjects. Subjects in the treatment group also show slight declines in resting sympathetic nerve activity (81.1± 5.19 bursts/100 heart beats vs 76.35± 5.97 bursts/100 heart beats) independent of changes in heart rate or baroreflex sensitivity. These preliminary results indicate a short course of respiratory training can lower daytime and nighttime blood pressures in adults with moderate obstructive sleep apnea these reductions may be mediated by changes in sympathetic nerve activity.

Funding: American Heart Association (Grant in Aid GRNT 26700007)

S8. Comparison of two phospho-mimic mutations of Cx43 with opposite arrhythmogenic potential

José F. Ek Vitorín, University of Arizona, Tucson, AZ , Tasha K. Pontifex, University of Arizona, Tucson, AZ, Janis M. Burt, University of Arizona, Tucson, AZ

Gap junction (GJ) channels are intercellular conduits crucial for cardiac impulse propagation and coordinated contraction. Channels formed by Connexin 43 (Cx43, the main ventricular GJ protein) are regulated by multiple kinases. At the intercalated disk (ID) of normoxic tissues, Cx43 appears phosphorylated in its carboxyl terminus by casein kinase 1 (CK1). During ischemia or pressure-overload-hypertrophy, CK1-phosphorylation fades and Cx43 relocates from the ID to the lateral borders of myocytes (remodeling). These alterations correlate with myocardial vulnerability to arrhythmia. Recently, it was shown that transgenic mouse hearts expressing Cx43 with CK1-phospho-mimicking mutations resist pathological remodeling and arrhythmia, while those expressing Cx43 with CK1-dephospho-mimicking mutations are more vulnerable to both remodeling and arrhythmia. Using patch-clamp in cell pairs, we explored the mechanistic basis for the arrhythmogenic character of these phospho-forms, assessing channels and junctions composed of Cx43 mutants wherein CK1-targeted serine residues (325, 328 and 330) were replaced by aspartate (Cx43-CK1-D) or alanine (Cx43-CK1-A) to mimic phosphorylation and dephosphorylation, respectively. Cx43-CK1-D GJs displayed multiple channel amplitudes, some larger ($\square j > 150pS$) than those typical of Cx43 wild type (WT), and strong junctional voltage-induced closure (Vj-gating). In contrast, Cx43CK1-A GJs displayed a shorter range of channel amplitudes ($\square j < 150pS$) and weak Vj-gating. The permselectivity (permeability to dyes/gj) of Cx43-CK1-D is similar to Cx43WT, while that of Cx43-CK1-A remains unknown. Surprisingly, both mutants are resistant to acidification, with Cx43-CK1-D displaying delayed uncoupling and Cx43-CK1-A being pimpervious to low-pH (~6.0). Both mutants display readily open hemichannels (HCh, undocked connexin hexamers) at depolarizing voltages. These data imply that the resistance to arrhythmia of hearts with CK1-phospho-mimicking Cx43 has a more nuanced underpinning than simply GJ resistance to acidification-induced closure or HCh activity. Possibly, phosphorylation at other sites that also confer cardioprotection in ischemic contexts have adjunct roles in the functional outcomes of the CK1-phosphomimic mutants. Data support a model whereby voltage gating, chemical gating and permselectivity of Cx43 GJ channels involve different, phosphorylation-dependent, structural conformations of the interacting domains of Cx43.

Funding: NIH

S9. Respiration is a one way street: Abdominal pumping induces unidirectional flow in beetles

Trevor P. Fox, Arizona State University, Tempe, AZ , Jon F. Harrison, Arizona State University, Tempe AZ

In insects, one of the important questions concerning air flow through the tracheal system is whether it is tidal, like mammals, or uni-directional as characterized by birds. Depending on the species and physiological conditions, gas exchange in insects can be mostly diffusive, tidally advective, or uni-directionally advective. To determine if unilateral, advective airflow is occurring in Zophobas moria beetles, we used a means of measuring abdominal gas exchange independently from thoracic gas exchange, with the hypothesis that pumping movement in the abdomen would drive air in a cohesive direction through the animal. To test this, the animals were divided in half using a latex membrane, with each half of the animal surveyed for CO2 output independently. We found that most animals display unidirectional flow either to the anterior mesothoracic spiracles, or to the posterior abdominal spiracles. T-tests between mean VCO2 thoracic and VCO2, abdominal were used to test for the disparity, confirming that most of the airflow was traveling in one direction. This indicates that unidirectional flow is occurring, albeit with some leakage of CO2 through the non-dominant spiracles. Considering these results, we believe that respiration in these animals is assisted by contractive and expansive pumping of the abdominal cavity, which compresses the trachea, causing adjective airflow through the animal.

S10. Doxorubicin temporally modules cyclooxygenase-2 levels in human vascular smooth muscle cells

***Gonzales RJ, University of Arizona, Phoenix, AZ ,** Tat T, University of Arizona, Phoenix, AZ , So M, University of Arizona, Phoenix, AZ , Bartel R, Arizona State University, Tempe, AZ , Sweazea K, Arizona State University, Tempe, AZ

Doxorubicin (Dox) is a chemotherapeutic agent that is highly effective at reducing recurrence and mortality in breast cancer patients. However, this anti-cancer drug elicits dose- and time-dependent cardiovascular toxicity. The pathogenesis of Dox is multifactorial, one of which involves the development and progression of inflammation mediated by activation of the TLR4/NFkB pathway. In a recent collaborative study, we demonstrated that intermittent bouts of Dox administered to mimic chemotherapeutic administration clinically attenuated protein levels cyclooxygenase-2 (COX-2), a downstream proinflammatory mediator of the TLR4/NFkB pathway, in cerebral and peripheral vasculatures isolated from female ovariectomized rats. These findings were surprising and not in agreement with previously published data. Therefore, to address whether this Dox-induced attenuated inflammatory response is time and dose dependent, we exposed cultured primary human female coronary and male aortic vascular smooth muscle cells to vehicle or Dox (0.3, 1.0, and 5 μM) for 6 and 24 hr. Following Dox treatment, cells were isolated, homogenized, and whole cell lysates analyzed for COX-2 protein levels via immunoblotting. In some experiments we also assessed NFkBp65 protein levels and or activation. We observed that Dox dose dependently decreased levels of COX-2 without altering NFkBp65 protein levels at the 6 h time point. However, at the 24 h time point Dox increased COX-2 levels and this was only noted at the highest Dox dose, 5 μM. NFkBp65 levels were not altered at the 6 h time point, however NFkBp65 translocation, measured indirectly using nuclear/cytosolic fractionation, was increased. At the 24 h time point NFkBp65 levels (whole cell lysate) were decreased only at the highest dose (5 μM) where COX-2 protein levels were elevated. Dox had no effect on cell morphology or density determined by light microscopy. Live vs. dead cell percentages determined using trypan blue were also not affected by Dox suggesting that the anticancer drug did not alter cell death at 6 and 24 h time points. In conclusion, studies demonstrate a possible novel action for the anticancer agent eliciting both a dose and time dependent effect on selective downstream mediators of inflammation such as COX-2 in the female and male vasculature. Future studies are planned to evaluate the impact of acute vs. chronic Dox treatment on COX-2 at the transcriptional or translational level to determine the mode of molecular regulation and to assess if sex differences exist.

Funding: University of Arizona Sarver Heart Center (MS) and the Valley Research Partnership P1 Grant (RG and MS)

S11. Targeted Metabolic Profiling of Bile Acids in Breast Cancer Patients

Wang D, University of Washington, Seattle, WA , Raftery D, University of Washington, Seattle, WA , Gu H, Arizona State University, Phoenix, AZ

In this study, we report on the development and application of a targeted metabolic profiling method for the quantification of bile acids (BAs) using plasm samples from healthy controls and breast cancer patients. , We carried out liquid chromatography-triple quadrupole-mass spectrometry (LC-QQQ-MS) scanning under multiple reaction monitoring (MRM) mode to profile 55 BA standards and 5 deuterated BA internal standards. We then quantified 55 BAs from plasm samples of 176 breast cancer patients and 92 healthy controls. Student's t-tests were conducted to analyze the differential metabolites between breast cancer patients and controls. A multivariate model based on partial least-squares-discriminant analysis (PLS-DA) was also used to distinguish breast cancer patients and controls. All plasma samples were obtained from Bloodworks Northwest and the Fred Hutchinson Cancer Research Center Breast Specimen Repository. Patient samples in this study were analyzed in accordance with the protocols approved by the University of Washington Institutional Review Board. , The developed method allows the quantification of 35 non-conjugated, 9 glycine-conjugated, and 11 taurine-conjugated BAs, using 5 additional deuterated BAs as internal standards, in a single analytical run with high

reproducibility. Among these 55 BAs, there were 24 BAs detected in plasm samples of breast cancer patients and healthy controls. In our preliminary analysis, 3 of these BAs showed statistical significance between the two groups ($p < 0.05$), Levels of all 3 BAs in the cancer group were lower than those in the control group. The resulting PLS−DA model was able to separate breast cancer patients from healthy controls in this study. , This targeted metabolomics approach provides a valuable tool with potential applications in many research areas focusing on BAs, including the discovery of diagnostic biomarkers and insights into the molecular pathogenesis of diseases. On the basis of these findings, this analytical method should provide new insights into the circulating BA pool in breast cancer patients as well as the study of a variety of diseases affected by BAs. Applications in biomarker discovery could furthermore provide guidance for clinical diagnosis and investigations of molecular pathogenesis in breast cancer.

Funding: Arizona State University Startup Funding (Haiwei Gu)

S12. Function of novex-3, the tiny titin in cardiac and skeletal muscle

***Kellermayer D, University of Arizona, Tucson, AZ ,** Smith JE3rd, University of Arizona, Tucson, AZ , Kiss B, University of Arizona, Tucson, AZ , Granzier H, University of Arizona, Tucson, AZ

Titin is a giant multi-functional striated muscle protein that is the third most abundant muscle protein after myosin and actin. The complete sequence of the titin gene contains a novel exon (novex) coding for the I-band sequence, named novex-3. The novex-3 transcript contains a stop codon and polyA tail signal, resulting in an unusually small (~700 kDa) isoform, referred to as novex-3 titin. This 'tiny titin' isoform extends from the Z-disc to novex-3 and is expressed in all striated muscles. Biochemical analysis of novex-3 titin shows that obscurin binds to novex-3 titin. The C-terminal domains of obscurin participate in signaling pathways of multicomponent protein complexes associated with calcium, SH3 and GTPase. Therefore, the novex-3/obscurin complex may act as a biochemical sensor and may have a role in hypertrophy and atrophy signaling pathways. Even though the full-length titin isoforms are widely investigated, the function of novex-3 titin isoform is poorly understood. My aim is to investigate the function and structure of novex-3 titin in cardiac and skeletal muscle and its interaction with obscurin. To examine the functional properties of novex-3 and the effects of skeletal muscle atrophy on novex-3 titin, C57BL6/J mice were introduced to hidlimb suspension (HS), a widely accepted ground-based model to study disuse atrophy in rodents. Mice were divided into HS, HS+reloading (RL) and control groups. The HS group was exposed to a 7-day-long suspension period. The HS+RL mice underwent 7 days of HS and a 7-day-long RL. After the completion of the HS and HS+RL protocols the mice were sacraficed and tissue weights were measured. Western blot analysis was performed to evaluate novex-3 and obscurin expression in different muscle types. We performed super-resolution microscopy (SIM) to analyze the location of novex-3 titin in the sarcomere. Muscle weights of the HS group were significantly lower compared to the control group. The tissue weights were increased in the HS+RL group compared to HS mice. Western blot analysis of cardiac and skeletal muscle shows that novex-3 and obscurin expressions are reduced in the HS group vs. control and are increased in HS+RL mice. SIM analysis revealed that the novex-3 distance from the Z-disk is ~300 nm and novex-3 extends when the sarcomere is stretched. In conclusion, hindlimb suspension affects the expression of novex-3 and obscurin in striated muscle. Moreover, the novex-3/obscurin complex localizes to the Z-disc region and may regulate calcium, and SH3- and GTPase-associated myofibrillar signaling pathways. We speculated that novex-3 titin could be involved in stress-initiated sarcomeric restructuring.

Funding: Interdisciplinary Training in Cardiovascular Research T32 HL007249 (DK) , National Institutes of Health grant HL062881 (HG) and HL118524 (HG)

S13. Proteome differences of subsarcolemmal and intermyofibrillar mitochondria reveal energy metabolism redistribution in skeletal muscle of obese subjects

***Kras KA, Arizona State University, Tempe, AZ ,** Langlais PR, University of Arizona, Tucson, AZ , De Filippis E, Mayo Clinic, Scottsdale, AZ , Roust LR, Mayo Clinic Scottsdale, AZ , Katsanos CS, Arizona State University, Tempe, AZ

Skeletal muscle is largely responsible for regulating whole body energy metabolism. Mitochondrial dysfunction and dysregulation of energy metabolism is implicated in the etiology of obesity. The reticular arrangement of mitochondria (MITO) within skeletal muscle provides the ability to rapidly transfer energy from one region to another. We sought to investigate the differences in proteome of skeletal muscle mitochondria (MITO) responsible for energy metabolism regulation and management of energy transfer throughout the reticulum, between lean and obese individuals. We hypothesized obesity would result in a reduction in the abundance, as well as a redistribution of mitochondrial proteins, within the mitochondrial reticulum, involved with regulating energy metabolism and associated biological pathways. Here we demonstrate a remodeling of mitochondrial reticulum in obese individuals. We isolated subsarcolemmal and intermyofibrillar mitochondrial fractions from vastus lateralis muscle biopsies using standard differential centrifugation techniques, from sedentary lean (n=16; 9M/7F) and obese (n=17; 9M/8F) subjects (age: 33±3 vs 31±2 years, mean±SE, $P > 0.05$; BMI: 23±1 vs 34±1 kg/m2, $P < 0.05$; Matsuda insulin-sensitivity index: 10.1±1.5 vs 4.2±0.8, $P < 0.05$). Our study identified 674 and 550 mitochondrial specific proteins, identified with at least two peptides in SS MITO and IMF MITO, respectively. We found 32 and 11 mitochondrial proteins from either SS MITO or IMF MITO, respectively, exhibiting differential expression between lean and obese individuals. Upon further analysis by Reactome.org, we demonstrate downregulation of the following mitochondrial biological pathways ($q < 0.01$) in the SS MITO and IMF MITO in obese subjects: citric acid cycle (TCA), electron transport chain (ETC), amino acid metabolism, and pyruvate metabolism. Additionally, we show the downregulation of mitochondrial biological pathways ($q < 0.01$) specifically in IMF MITO from obese subjects: ATP synthesis and heat production by uncoupling. Finally, our study shows the relative distribution of proteins associated with mitochondrial proton-motive force production in the cell periphery (i.e. SS MITO) is not different between lean and obese. However, the relative distribution of proteins associated with mitochondrial proton-motive force utilization for ATP production in the cell interior (i.e. IMF MITO) near contractile and transport ATPases, is lower in obese subjects. Overall our findings suggest obesity results in energy metabolism redistribution within the skeletal muscle mitochondrial reticulum.

Funding: Grant #: R01DK094062

S14. INCREASED SERUM GIP LEVELS CORRELATE TO IMPROVED SURVIVAL RATES IN FEMALE DF508-CF MICE FED DIETARY GENISTEIN

***Ryan Lord,** Taylor Bowman, Archana Chandrashekar, Nathan Fairbourn, Charisma Mylavarapu, Ammer Dbeis, & Craig Hodges and Layla Al-Nakkash

The most common clinically seen mutation in cystic fibrosis (CF) is DF508. Mice homozygous for the DF508 mutation have severe intestinal disease and require constant laxative (Colyte) treatment for survival. This pathology mimics the intestinal obstruction (meconium ileus) seen in 6-20% of CF patients. The purpose of this study was to determine whether dietary genistein would reduce the dependence of the DF508 CF mouse on laxatives for survival and improve mortality rates. Genistein is a naturally occurring isoflavone found in soy. At age 21 days, DF508 mice were maintained on one of three diets for 45 days post weaning; regular diet, regular diet + Colyte, or genistein diet (600G). Survival rates for each diet group were; males fed normal diet = 38% (8/21 mice), males fed normal diet + Colyte = 83% (35/42 mice), males fed 600G = 60% (9/15 mice) and females fed normal diet = 47% (9/19 mice), females fed normal diet + Colyte 71% (27/38 mice), females fed 600G = 87% (13/15 mice). Body weight at the end of the diet study was 16% greater in males fed 600G versus those on Colyte (with no change in final weight gain in the female groups). In order to assess how dietary genistein may improve survival or

weight gain, we examined the following: (1) histomorphometric analyses to examine changes in jejunum villi length/crypt depth/wall thickness, numbers of goblet cells, (2) western blot analyses to investigate differences in protein expression of key jejunum epithelial transporters (Glut2, Glut5, SGLT1), and (3) serum profile of GIP, insulin, glucose, resistin. We conclude that feeding DF508 mice genistein (600G) diet for 45 days; (1) abolished the dependence on laxatives for survival in females, (2) significantly increased serum GIP levels in females, (2) significantly increased serum glucose levels in females and males, (4) significantly increased weight gain in males. These studies could have impact on clinical interventions to improve growth and survival in patients.

Funding: Archana Chandrashekar and Charisma Mylavarapu was supported by the MWU Summer DO Fellowship Program. Layla Al-Nakkash was supported by: Soy Health Research Program, Diabetes Action Research & Education Foundation and MWU Intramural funds.

S15. Heat production deficiencies in the muscular dystrophy with myositis (mdm) mouse

***Miyano CM, Northern Arizona University, Flagstaff, AZ ,** Fernandez Orezzoli S, Northern Arizona University, Flagstaff, AZ , Buck CL, Northern Arizona University, Flagstaff, AZ , Nishikawa KC, Northern Arizona University, Flagstaff, AZ

Homeothermic animals, including birds and mammals, strive to maintain core body temperature across varying ambient temperatures. Mice with the muscular dystrophy with myositis (mdm) mutation are heterothermic and unable to maintain their body temperature. Mdm mice are characterized by a deletion in the N2A region of titin, a spring-like protein in muscle, resulting in a lower body mass, stiffer gait, and reduced lifespan. Additionally, they shiver at a lower than expected frequency, and have reduced active muscle stiffness and increased passive muscle stiffness in vivo compared to wild type mice. The underlying defect that leads to a lower shivering frequency is not known but could be caused by changed muscle stiffness. The purpose of this study was to evaluate potential causes for the inability of mdm mice to maintain homeothermy during cold stress. The inability to defend their body temperature could be due to the N2A deletion in the titin protein, leading to a more compliant spring and a lower shivering frequency. An alternative hypothesis is that the ability of mdm mice to use nonshivering thermogenesis, a mechanism in brown adipose tissue that generates heat, is impaired. Mice underwent a 4-day cold stress experiment that used a continuous system for indirect calorimetry, a method that measures respiratory gases to determine heat production in the form of metabolic rate. The cages were placed in an incubator so that ambient temperature could be controlled to either 34, 29, 24, or 19 degrees C for each experiment. Upon conclusion of the cold stress experiment, norepinephrine-stimulated thermogenesis was employed by administering 1.2 mg/kg of norepinephrine. Metabolic rate, core body temperature, and thermal conductance were measured in wild type and mdm mice during both experiments. Mdm mice increased metabolic rate during the cold challenge at all but the lowest temperature (19 degrees C). Core body temperature for mdm mice decreased with decreasing ambient temperature within a range of 28 – 37 degrees C. During norepinephrine-stimulated thermogenesis, both groups increased their oxygen consumption with no difference between groups. These results suggest that mdm mice do not increase their capacity for nonshivering thermogenesis and that heterothermy is likely due to reduced efficiency of shivering thermogenesis, possibly related to spring properties of titin.

Funding: Our funding sources include NSF IOS-0742483, NSF IOS-1025806, and NSF IOS-1456868, the W. M. Keck Foundation, and the Technology Research Initiative Fund of Northern Arizona University.

S16. Effects of Detraining and Retraining in a Follow-Up Cohort With Type 2 Diabetes

***Ojameruaye O, Northern Arizona University, Phoenix, Arizona, USA ,** Hornsby BC, Northern Arizona University, Flagstaff, Arizona, USA , Wilson G, University of Otago, Dunedin, New Zealand , Baldi JC, University of Otago, Dunedin, New Zealand

The purpose of this study was to assess the effects of detraining and retraining on aerobic capacity (VO2max), heart rate recovery (HRR), and max power in a follow-up cohort of non-diabetics (ND) and type 2 diabetics (T2D) and also monitor exercise adherence. We hypothesized that VO2max, HRR, and max power will decrease with detraining and be restored after retraining in both groups and that adherence will be greater than 80% attendance and 90% effort. Six medically stable adults (4 ND, 2 T2D) were recruited from a preceding study. Max testing and exercise sessions were conducted at Dunedin Hospital and The University of Otago Physical Education training lab. Max test was performed using incremental exercise on a cycle ergometer while monitoring metabolic variables (CPET, COSMED). Our intervention consisted of 12 sessions (two weeks) of high-intensity interval training (HIIT) at an intensity of at least 90% of age predicted heart rate max (AP-HRmax). A polar heart rate monitor was used to monitor heart rate during exercise. Results of our study showed a total drop in VO2max and HRR (4%), and max power (5%) with detraining. Retraining resulted in a total drop of 1% in VO2max, 7% in HRR, and a 2% increase in max power. Compared to the ND group, the drop in VO2max in the T2D group was more pronounced with detraining (2% vs 10%). This trend continued in the ND group (2%) but was negligible in the T2D group after retraining. HRR dropped with detraining (ND= 5%, T2D= 2%) and dropped even more following retraining in T2D (11%), but leveled off for ND. Compared to the ND group (2%), the drop in max power in the T2D group (14%) was more pronounced with detraining. Post-retraining max power did not change in the ND group and increased in the T2D group (8%). Adherence was higher in the T2D group (total= 79% attendance, 100% effort; T2D= 100% attendance, 100% effort; ND= 69% attendance, 100% effort). The results of this study show that a 12-session intensive HIIT program was insufficient in eliciting positive changes in the measures of interest besides max power in the T2D group. We also showed that these key variables are more sensitive to detraining in the T2D group.

Funding: National Institute On Minority Health And Health Disparities of the National Institutes of Health under Award Number T37MD008626.

S17. GABAergic neurons in vocal- and non-vocal learning hummingbirds

Bernier, K, Midwestern University, Glendale, AZ , Potter, RM, Midwestern University, Glendale, AZ , ***Olson, CR, Midwestern University, Glendale, AZ**

GABA is the main inhibitory neurotransmitter in vertebrates and plays fundamental roles in motor and sensory forebrain processing. We identified GABA expression in vocal learning (Costa's, *Calypte costae*) and non-vocal learning (black-chinned, *Archilochus alexandri*) hummingbirds, and compared it to that of the zebra finch (*Taeniopygia guttata*), a well-studied songbird that evolved vocal learning independently of hummingbirds. We used *in situ* hybridization to label inhibitory interneurons with a riboprobe for GAD2, a marker of GABAergic cells that is well described in the finch model. In our hands, GAD2 expression matched that of previous work in the finch, and its expression was present in the brains of both hummingbirds. Similar to patterns in the finch, GAD2 was prominent in the Costa's forebrain and enriched in striatum, showing regional heterogenicity in inhibitory neural subtypes. The vocal circuitry of Costa's hummingbird (confirmed with darkfield imaging) revealed a subpopulation of large-bodied GAD2-positive cells with enriched expression in the hummingbird analogs of RA, HVC and LMAN. However, these larger cells are absent in adjacent neural tissue. Compared to the finch model, GAD2-positive cells appear to have greater prominence in the vocal circuitry of the Costa's hummingbird. Yet, while black-chinned hummingbirds had GAD2 expression that was broadly similar to that of the Costa's and finch,

a major difference is that the prominent GAD2-cells of vocal nuclei were absent. These results suggest that enhanced GABAergic signaling is a critical component of vocal production, and suggests that among the hummingbird lineages that possess vocal learning, employing a strategy of enhanced neural inhibition within the vocal circuit was a necessary component.

Funding: MWU Faculty Startup

S18. An extended matched filter between call frequency and auditory sensitivity in northern grasshopper mice

Green D, Northern Arizona University, Flagstaff, AZ , Scolman T, Northern Arizona University, Flagstaff, AZ , **Pasch B, Northern Arizona University, Flagstaff, AZ**

Vocal communication is a critical component of mate attraction and territorial advertisement in a variety of taxa. Optimality theory predicts a strong match between signal properties of senders and hearing sensitivity of receivers, but morphological or physiological constraints may reduce tight correspondence. We recorded vocalizations and measured auditory brainstem responses (ABR) – a physiological measure of hearing sensitivity – in northern grasshopper mice (Onychomys leucogaster), a species that produces long-distance calls to advertise their presence to rivals and potential mates throughout arid regions of the western United States. ABR data indicate heightened sensitivity (32.5 ± 2.0 dB SPL re: 20 uPa) to tones between 10 kHz and 12 kHz (n=10), which correspond to the fundamental frequencies (11.6 ± .63 kHz, n=36) of long-distance calls produced by senders. Interestingly, peak hearing sensitivity extends to higher frequencies, potentially indicating selection for detection of congeners that co-occur with O. leucogaster. Our findings provide support for the matched filter hypothesis but extend this paradigm to ecologically relevant social contexts.

Funding: Northern Arizona University, Animal Behaviour Society

S19. Lenalidomide attenuates high fat diet induced cyclooxygenase-2 levels in primary human vascular smooth muscle cells

***Rahman S, University of Arizona, Phoenix AZ ,** Bartel R, Arizona State University, Tempe AZ , DeCourt B, Arizona State University, Tempe AZ , Sweazea KL, Arizona State University, Tempe AZ , Gonzales RJ, University of Arizona, Phoenix AZ

Lenalidomide is a derivative of thalidomide and is currently used as a drug to treat multiple myeloma cancer. It is known to inhibit cytokines such as TNF-alpha and IL-6. Results from others suggest that through the inhibition of these cytokines that oxidative stress as a result of exposure to high fat exposure can be reversed. In previous studies it has been determined that exposure to palmitic acid, a saturated and high density fat, results in oxidative stress and an inflammatory response in cells. It's hypothesized that increased oxidative stress and inflammation occurs as a result of enhanced production of reactive oxygen species (ROS). The level of inflammation can be determined by analyzing the level of protein expression of the pro-inflammatory enzyme, cyclooxygenase-2 (COX-2). In this study primary male aortic vascular smooth muscle cells at passage 7 were treated with vehicle (bovine serum albumin and dimethyl sulfoxide in cell culture buffer), 100 uM palmitate, lenalidomide (0.5, 1.0, or 5 uM), and 100 uM palmitate plus 0.5, 1.0, or 5 uM lenalidomide for 18 h. Following the drug treatment, cells were isolated, homogenized, and analyzed for COX-2 expression levels using western analysis. Consistent with previous data, our human vascular smooth muscle cells basally express COX-2. Following palmitic acid administration COX-2 levels were increased. Lenalidomide alone had a small increase of expression of COX-2 compared to the vehicle. In addition with palmitic acid, lenalidomide reduced the pal-induced increase in COX-2 levels suggesting that lenalidomide may have some ability to reverse palmitate induced vascular inflammation. In conclusion, lenalidomide may function to reduce the inflammation which is a product of high fat conditions. Future studies

and further analyses will include an assay to determine TNF-alpha expression in the cells, and also an assay to measure the amount of ROS in the cells.

Funding: Valley Research Partnership P1 (RG)

S20. Studying amphibian physiology to evaluate pesticide safety in rice fields.

Molly E. Shuman Goodier - Department of Biological Sciences, Northern Arizona University, Flagstaff, AZ, 86001, Grant Singleton- International Rice Research Institute, Los Baños, Philippines, Shyann Hinesa* - Undergraduate Researcher, Department of Biological Sciences, Northern Arizona University, Flagstaff, AZ, 86001 , Catherine R. Propper - Department of Biological Sciences, Northern Arizona University, Flagstaff, AZ, 86001

The pollution of water resources due to the intensification of modern rice agriculture and corresponding increase in pesticide use poses a threat to biodiversity and human health. Amphibian species represent valuable indicators within this system because they utilize rice paddies as habitat in the absence of natural wetlands, and pesticide applications coincide with reproductive and developmental cycles. We conducted an experiment with wild Rhinella marina tadpoles at the International Rice Research Institute (IRRI) in the Philippines to 1) test whether environmentally relevant exposure to butachlor, an acetanilide herbicide used extensively in rice fields throughout Southeast Asia, affects development and thyroid physiology, 2) determine which developmental stages are most vulnerable to exposure, and 3) test the degree to which tadpoles are able to acclimatize to sub-lethal exposure. Our analysis revealed that R. marina exposed to butachlor developed slower and weighed less, and that some concentrations affected the development of the thyroid: exposed individuals had fewer thyroid follicles and smaller thyrocyte cells. Furthermore, we found that R. marina eggs were more sensitive to exposure than tadpoles, and we observed evidence of acclimatization: animals exposed to butachlor early in life performed better than naïve animals during a second exposure. Our findings support recent work indicating that butachlor causes thyroid endocrine disruption in vertebrates, and suggest that realistic exposure in rice fields presents a concern for wildlife and human health. Furthermore, because R. marina is a widespread invasive species and highly abundant within rice fields, we suggest using it to assess consequences of realistic exposure to pesticides in tropical countries where it has been introduced.

Funding: Closing Rice Yield Gaps in Asia with a Reduced Environmental Footprint (CORIGAP) funded by the Swiss Agency for Development and Cooperation , Achievement Rewards for College Scientists (ARCS) Foundation

S21. Cytochrome C Oxidase is Differentially Methylated in Whole Blood from Participants with Metabolic Syndrome

***Keane P. Urashima, University of Arizona, Tucson, AZ ,** Anastasia M. Miramontes, University of Arizona, Tucson, AZ , Jonathan D. Roe, University of Arizona, Tucson, AZ , Erika Krall, University of Arizona, Tucson, AZ , Luis A. Garcia, University of Arizona, Tucson, AZ , Dawn K. Coletta, University of Arizona, Tucson, AZ

The metabolic syndrome is comprised of a number of diseases including obesity, dyslipidemia, hypertension, and glucose intolerance. It is caused by genetic and environmental factors. However, epigenetic mechanisms of the metabolic syndrome are less well known. DNA methylation provides a mechanism whereby environmental factors can influence gene transcription. The aim of our study was to investigate human whole blood DNA methylation of cytochrome c oxidase subunit 6C (COX6C) in participants with and without metabolic syndrome. All participants (n=184) were Latino descent from the Arizona Insulin Resistance registry. Subjects were classified based on the metabolic syndrome phenotype according to the National Cholesterol Education Program's Adult Treatment Panel III. Of the 184 Latino participants in the study, 74 were classified with the metabolic syndrome (MetS-Yes) and 110 were without (MetS-No). Genomic DNA was extracted from the blood samples with the PAXgene DNA extraction

kits. The DNA samples underwent bisulfite conversion via the Zymo EZ DNA methylation lighting reagent kit. COX6C was amplified using the primer set from the Qiagen Hs_COX6C_01_PM PyroMark CpG assay. Pyrosequencing was performed on the Qiagen Q48 Autoprep utilizing the sequencing primer from the Hs_COX6C_01_PM PyroMark CpG assay. In total, there were four CpG positions captured using this assay. Of these, we showed that Chr8:100,905,761 (MetS-No: 1.4% (SEM=0.093) versus MetS-Yes: 0.9% (SEM=0.104), $P < 0.05$) and Chr8:100,905,787 (MetS-No: 2.5% (SEM=0.135) versus MetS-Yes: 1.7% (SEM=0.153), $P < 0.05$) were significantly decreased in methylation in the participants with metabolic syndrome. In a previous study, we had shown an increase in the mRNA expression of COX6C in MetS-Yes (+1.6 fold change) versus MetS-No (Tangen et al, 2013). Our results demonstrate that COX6C, a mitochondrial regulatory subunit of cytochrome c oxidase is differentially methylated in metabolic syndrome participants. Moreover, we demonstrate that there is a negative correlation between COX6C methylation and gene expression in metabolic syndrome participants.

Funding: This study was supported in part by a NIDDK grant: R01DK094013 (DKC)

S22. Predicting in vivo muscle force in running guinea fowl using a muscle model based on the winding filament hypothesis.

Whitney, CD, Northern Arizona University, Flagstaff AZ, Daley, MA, Royal Veterinary College, London, UK

Although a large amount of effort has been put towards modeling muscle forces, muscle models are still unable to predict forces during dynamic animal movements, especially with perturbations (e.g. moving over obstacles). In this study, we use a novel model inspired by the winding-filament hypothesis to predict muscle forces in running guinea fowl. Lateral gastrocnemius lengths, activations and forces were measured using sonomicrometry, implanted EMG, and tendon buckles, respectively. Guinea fowl (n = 2) were recorded running on a treadmill during level running and running over 5cm and 7cm obstacles. Muscle morphology parameters included pennation angle, muscle mass and muscle fascicle resting length. The EMG was smoothed, transformed to a percentage of maximum activation, and shifted by a time delay to account for excitation-contraction coupling. The winding filament model (WFM) consists of a contractile element in series with a spring. The contractile element is also in series and parallel with a second spring and damper, representing the titin protein, which wraps around a pulley representing actin thin filaments. Muscle length and activation are inputs to the model, and muscle force is predicted in each time step. The predicted forces were compared to measured forces. The free parameters (n = 6), including an activation factor that varied from trial to trial, were optimized locally and globally using a high-performance computer. Results show that the WFM-based model more accurately predicts forces during perturbed and level gaits ($R2 = 0.72$-0.86) than published results using complex Hill-type models. Biological relevance of the model was assessed by evaluating input parameters, internal model variables, and sensitivity analysis.

Funding: Hooper Undergraduate Research Award

S23. Troponin I phosphorylation in diabetic and non-diabetic hearts

***Wilson TJ, Northern Arizona University, Flagstaff, AZ ,** Erazo MN, Northern Arizona University, Flagstaff, AZ , Erickson JR, University of Otago, Dunedin, NZ

Diabetic heart dysfunction is an umbrella term that encompasses the group of cardiac issues correlated with diabetes. It has been hypothesized that these issues arise from calcium mishandling in the diabetic heart. Recently, our lab has shown that inhibition of CaMKII restored force development in trabeculae from diabetic rat hearts, moreover calcium transient amplitude and sarcoplasmic reticulum calcium load were unaltered in diabetes or by CaMKII inhibition. This finding led us to examine whether expression or phosphorylation was altered for the myofilament protein cardiac troponin I (cTnI), an important regulatory protein involved in

contraction and relaxation with key phosphorylation sites at Ser22/23 and Thr144. To test this hypothesis total cTnI, Ser22/23, and Thr144 protein levels were measured in diabetic and non-diabetic human right atrial appendages (RAA) using Western blots and IHC. There were no significant differences seen in Ser22/23 and Thr144 phosphorylation in either assay, although there was a trend towards significance. cTnI protein expression was significant in the non-diabetic <50% ejection fraction RAA in Western blots only. A limitation of this study was small sample size. Future studies with a larger n are suggested and could possibly lead to novel treatments for diabetic cardiac dysfunction.

Funding: The Minority Health International Research Training (MHIRT) program. Funding for this presentation was made possible (in part) by T37MD008626 from the National Institute on Minority Health and Health Disparities.

S24. A Role for the Brain Renin-Angiotensin System (RAS) in Parkinson's, Alzheimer's, and Down syndrome

***Zawada WM (1),** Palmer Q (2), Jones R (2), Biedermann J (2), and Griffin WST (2). , 1. A.T. Still University, School of Osteopathic Medicine Arizona (SOMA), Mesa, AZ 85206 , 2. Reynold's Institute on Aging, University of Arkansas for Medical Sciences, Little Rock, AR 72205.

Neuronal stress and activation of neuroinflammatory and angiotensin cascades are common across a range of neurodegenerative diseases including Parkinson's, Alzheimer's, and Down syndrome (DS). We found that excessive activity of the brain RAS is associated with poor neuronal survival in models of neurodegenerative diseases. Searching for the physiological mechanisms responsible, we chose to examine the earliest molecular events taking place in the brain just hours after initiation of neuronal injury. To model such acute activation of stress cascades, we injected a neurotoxin, MPTP, intraperitoneally (4x/2hrs apart) in male C57 mice. The neurotoxin is thought to incite some of the cellular stresses similar to those found in the brains of Parkinson's disease (PD) patients. MPTP affected transcription in the brain by: i) decreasing tyrosine hydroxylase mRNA, a bellwether of function of dopamine neurons; ii) modifying transcription of renin angiotensin system genes by increasing angiotensin II (Ang II) type 1 receptor (AT1R) mRNA (a driver of NADPH oxidase (Nox)-mediated superoxide production) and decreasing AT2R mRNA (a neuroprotective receptor that counteracts AT1R); iii) increasing the levels of Nox4 and IL-1β mRNA; and iv) increasing levels of α-synuclein mRNA. Pretreatment of mice with Telmisartan, an AT1R antagonist, led to a reduction in several neuronal stress signatures, including α-synuclein, AT1R, β amyloid precursor protein (βAPP), and S100B, all of which are elevated by MPTP. These pathological changes may be important beyond Parkinson's as we observed that neurons in sections from DS fetuses have elevated Nox4 and glia have elevated IL-1. Because phosphorylation-dependent activation of mitogen-activated protein kinases (MAPKs) is necessary for cytokine and Nox actions, we are now exploring interactions between brain RAS and an important terminator of neuroinflammatory and neurooxidative cascades, MAP kinase phosphatase-1. Because Telmisartan prevents MAPK mediated inflammation and apoptosis, studies on the Telmisartan-mediated regulation of these processes in neurodegenerative conditions are warranted. In summary, in our MPTP-induced model of neuronal stress, Telmisartan demonstrated an extraordinary ability to prevent most of the pathological changes characteristic of neuronal injury, suggesting that Telmisartan acts to maintain or restore normal neuronal physiology in the face of severe neuronal stress. Repurposing AT1R antagonists like Telmisartan to modify angiotensin signaling, and thereby quell neuronal stress, may offer a novel therapeutic approach for PD and DS, which is a harbinger of Alzheimer's disease.

Funding: Supported by A.T. Still University (WMZ) and NIH P01 AG12411 (WSTG)

FRIDAY TALKS (NOT BEING PRESENTED AS POSTERS)

Session II. Comparative Physiology

Living on the human-wildlife boundary: determinants of activity in suburban striped skunks (Mephitis mephitis)

***Zhang VY, Northern Arizona University, Flagstaff, AZ ,** Theimer TC, Northern Arizona University, Flagstaff, AZ , Williams CT, Northern Arizona University, Flagstaff, AZ , Buck CL, Northern Arizona University, Flagstaff, AZ

The occurrences of human-wildlife conflicts will increase in frequency with the expansion of urban development. The ecology of a species, including their daily and seasonal patterns of activity, likely influence the temporal patterns of these conflicts with humans. Striped skunks (Mephitis mephitis) are common to urban and suburban landscapes across North America, but due to their nocturnal nature, the ecology of these populations is not well described. In this study, we used tri-axial accelerometers to continuously measure the overall dynamic body acceleration (ODBA), an index of activity-specific energy expenditure, in a suburban population of striped skunks across a one-year period. We used linear mixed effects models to determine the effects of various weather parameters on activity and also find differences of activity between sexes and across breeding stages. To understand the influence of reproductive state on the timing of daily activity, we examined the differences in onset times of daily activity bouts relative to civil dusk across the year. Weather influenced daily ODBA in both males and females, with the effects of various weather parameters dependent on breeding stage. Snow cover significantly decreased activity levels in both males and females, possibly due to low food availability. Seasonal differences in daily ODBA were consistent with metabolic and reproductive demands; females were most active during late-lactation, males were most active during mating, and activity increased in both sexes during spring/summer when compared to fall/winter. The onset times of daily activity in males did not vary across the annual cycle, while the onset times of daily activity in females coincided with daylight hours during mid- through late-summer. During this period, females might experience tradeoffs between diurnal predation risk and the high forage requirements for rearing young. Overall, we demonstrate how accelerometers can provide a minimally-invasive method for understanding the continuous movement patterns and activity-specific energy expenditure of free-living mammals; our data suggest that managers of urban wildlife should consider the importance of species activity patterns when developing management strategies.

Funding: Northern Arizona University, National Science Foundation Division of Integrative Organismal Systems, U.S. Department of Agriculture Animal and Plant Health Inspection Service

Functional hypoxia and HIF-signaling pre-molting in Drosophila

***Harrison, JF, Arizona State University, Tempe, AZ ,** Campbell, J., Arizona State University, Tempe, AZ , Cogley, T., Arizona State University, Tempe, AZ , Fox, T. Arizona State University, Tempe, AZ , Lindquist, T., North Dakota State University, Fargo, N.D. , Greenlee, K.J., North Dakota State University, Fargo, N.D.

An emerging concept is that insects may experience functional hypoxia prior to molting due to growth of oxygen-requiring tissues while oxygen delivery is limited by unexpandable portions of the respiratory system. Additonally, it has been proposed that this functional hypoxia may be an important trigger for molting in insects, and possibly generally in arthropods. However, data are conflicting as hyperoxic rearing does not increase size of all insects. We studied metabolism and hypoxia-inducible factor (HIF) related transcription in early and late- (pre-molt) 3rd instar Drosophila larvae, and found multiple lines of evidence supporting the occurrence of functional hypoxia appearing in pre-molt animals. In pre-molt (but not early instar animals), lactate levels increased, CO_2 emission rates increased in hyperoxic atmospheres, and copy number of the Drosophila homologs of HIFalpha, HIFbeta and

prolyl hydroxylase mRNA all increased, as did quantity of HIFalpha protein (Westerns). In pre-molt animals, hyperoxia suppressed gene expression of HIFalpha and prolyl hydroxylase, and hypoxia increased prolyl hydroxylase, supporting the hypothesis that the elevation in HIF signaling and lactate in premolt animals is due to functional hypoxia rather than an aerobic glycolytic patterns induced hormonally independent of hypoxia. RNAi-mediated knockdown of HIF signaling in the prothoracic glands, site of production of ecdysone (molting hormone), strongly delayed eclosion in 10% but not 21% oxygen atmospheres. Thus HIF-signaling in this endocrine gland appears to be an important component of how Drosophila ecloses at a smaller body size when reared under hypoxic conditions. However, the lack of an effect of knockdown of HIF signaling in normoxic atmospheres suggests that HIF-signaling in the prothoracic glands is not an important element in control of molting during normoxia.

Funding: Supported by NSF IOS 1256745.

SATURDAY TALKS (NOT BEING PRESENTED AS POSTERS)

Session V. Cutting-Edge Methods in Physiology

Non-conventional anoxia tolerance: adult Drosophila outlive larvae despite inferior ATP and hemolymph K+ maintenance.

***Campbell JB, Arizona State University, Tempe, AZ ,** Harrison JF, Arizona State University, Tempe, AZ

Oxygen limitation plays a key role in many pathologies, and yet we still lack a fundamental understanding of the mechanisms responsible for intra- and interspecific variation in hypoxia/anoxia tolerance. Current theory suggests that a better anoxia tolerance primarily involves the ability to maintain cellular energetic status as depletion of ATP leads to detrimental processes including the disruption of ionic homeostasis and depolarization of membranes. In this study, we tested for possible mechanisms that allow Drosophila melanogaster adults to survive longer periods of anoxia than late third instar larvae (LT50: ~8 vs. 1 h). Adults were quickly paralyzed (<30 sec) by anoxia , while larvae attempted escape for 30 min. During the first two hours, in larvae, ATP fell to 0.8% of normal and [K+] rose by 50%, and survival fell to zero in strong correlation with ATP and [K+]. In adults, during the first two hours, ATP to fell to 2% of normal values, [K+] increased by ~3x, but survival was 100%. During the next six hours, adults maintained high survival rates, while ATP was maintained at 2% of normal levels, and hemolymph [K+] continued to increase to ~5x normal levels. Over 8 h of anoxia, adults could quickly restore hemolymph [K+] levels if returned to normoxia, despite having hemolymph [K+] levels up to 4.5x greater than resting levels. In adults exposed to more than 8 h of anoxia, ATP levels decreased further and [K+] continued to rise, and both of these variables correlated tightly with decreased survival. The superior anoxia tolerance of adult D. melanogaster appears to be due to the capacity to maintain and tolerate very low but non-zero ATP levels, and to be able to tolerate extremely high extracellular [K+]. This study suggests that a new focus of research in anoxia-tolerance should be the mechanisms by which animals can survive and quickly recover from such energetic and ionic conditions. Supported by NSF IOS 1256745.

Funding: Supported by NSF IOS 1256745.

Session VI. History of Physiology

What I failed to learn in kindergarten or graduate school concerning the history of physiology

***Tipton, Charles M., University of Arizona, Tucson.**

Although the majority of kindergarten teachers emphasize physiological concepts in their health sessions; my mentors failed to cover the 1542 Physiologia text of Fernel; or the Cartesian beliefs of Descartes who proposed during the 16th century that humans functioned as machines. This belief was endorsed by the Royal Society of Physician in London from 1636-1666 as well as by the Oxford physiologists during the 17th century. Unfortunately, my mentor and likely others, never mentioned the 16th century Dutch manuscripts pertaining to Oeconomia Animalis written by Muis, Bontehoe, Charleston and Craamen, that contributed to human physiology plus nutritional principles. Surprisingly, I was never taught about the establishment of the School of Medicine at Montpellier, France that became as bastion of Vitalism between 1800 and 1850. This doctrine indicated life processes could not be explained by the Laws of physics or chemistry. Fortunately, because of the writings and texts of von Haller, Boerhaave, and Robinson, vitalism did not prevail, and modern physiology came into existence.